

**People's Democratic Republic of Algeria**  
**Ministry of Higher Education and Scientific Research**  
**University M'Hamed BOUGARA – Boumerdes**



**Institute of Electrical and Electronic Engineering**  
**Department of Electronics**

Final Year Project Report Presented in Partial Fulfilment of  
the Requirements for the Degree of

**MASTER**

**In Telecommunication**

**Option: Telecommunication**

Title:

**Ground Roll attenuation using  
(f, k) and AGORA filters**

Presented by:

- **Mohamed Salah NEKHOUL**
- **Yassine BADOUCHI**

Supervisor:

**Dr. Dalila CHERIFI**

Registration Number:...../2018

<b>Figure</b>	<b>Page</b>
<i>Figure 1.1. Geophone</i>	4
<i>Figure 1.2. Convolution between two signals</i>	5
<i>Figure 1.3. Process of the cross correlation</i>	6
<i>Figure 1.4. 2D seismic recording</i>	6
<i>Figure 1.5. 3D seismic recording</i>	6
<i>Figure 1.6. P wave</i>	7
<i>Figure 1.7. S wave</i>	8
<i>Figure 1.8. Love wave</i>	8
<i>Figure 1.9. Rayleigh wave</i>	9
<i>Figure 1.10. Seismic wave path</i>	9
<i>Figure 1.11. Geometrical Divergence</i>	11
<i>Figure 1.12. The different waves in seismic recording</i>	12
<i>Figure 1.3. Seismic Refraction geometry</i>	14
<i>Figure 1.14. Seismic multiple reflection</i>	14
<i>Figure 1.15. Static correction</i>	16
<i>Figure 1.16. Near-surface</i>	16
<i>Figure 1.17. Normal move-out correction</i>	18
<i>Figure 1.18. reflection event hyperbola</i>	19
<i>Figure 1.19. NMO correction, stacked traces</i>	19

Figure 1.20. Diagram showing the ray path for a zero-offset reflection 20

Figure 1.21. Diagram showing the ray path for a zero-offset reflection from a dipping reflector and the resultant apparent dip 21

Figure 2.1. Projection of a seismic section in the plan ( $f, k$ ) 27

Figure 2.2. Relation between ( $x-t$ ) and ( $f-k$ ) plans 27

Figure 2.3. GR velocity map with record locations, b-e) the corresponding shot records. 30

Figure 2.4: a) raw input central cable, b) filtered central cable, 31  
c) difference between a) and b) d) raw input broadside cable,  
e) filtered broadside cable, f) difference between d) and e)

Figure 2.5. Stack of the input data 32

Figure 2.6: Stack after an adaptive filtering of the GR on raw shots 32

Figure 2.7. Stack of the noise removed during the adaptive filtering 33

Figure 3.1. NEGRINE region Location. 34

Figure 3.3. 16GN04 profile location map of block 126 35

Figure 3.4. Elevation graph of the 16GN04 profile surface 35

Figure 3.5. geophones Arrangement in the field 37

Figure 3.6. RMS amplitude of the 16NG04 profile 37

Figure 3.7. Raw stack of the 16NG04 profile. 38

Figure 3.8. Stack of the 16NG04 profile after editing 38

Figure 3.9. Raw shot 1004 39

Figure 3.10. The shot 1004 after editing 39

Figure 3.11. Amplitude spectrum before editing and after. 40

Figure 3.12. Amplitude spectrum for the 16NG04 profile stack 41

before and after editing.

<i>Figure 4.13.</i> Location of spikes on shot 1004 after Edition	42
<i>Figure 3.14.</i> Shot 1004 after Despiking	43
<i>Figure 3.15.</i> Stack of the 16NG04 profile before Despiking	43
<i>Figure 3.16.</i> Stack of the 16NG04 profile after Despiking	44
<i>Figure 3.17.</i> Amplitude spectrum for shot 1004 before and after Despiking	45
<i>Figure 3.18.</i> The stack of 16NG04 profile shows the target area.	46
<i>Figure 3.19.</i> Representation of the different events on shot 1004 after the attenuation of the random noises.	46
<i>Figure 3.20.</i> Shot 1004 before (f, k) filtering.	48
<i>Figure 3.21.</i> Shot 1004 after (f, k) filtering.	49
<i>Figure 3.22.</i> Stack before (f, k) filtering.	50
<i>Figure 3.23.</i> Stack after (f, k) filtering.	50
<i>Figure 3.24.</i> Amplitude spectrum before and after (f, k) filtering.	51
<i>Figure 3.25.</i> Raw shot 1004 Representation in the (f, k) domain	52
<i>Figure 3.26.</i> Shot after (f, k) filtering in (f, k) domain.	52
<i>Figure 3.28.</i> Shot 1004 before AGORA.	53
<i>Figure 3.28.</i> Shot after AGORA.	54
<i>Figure 3.29.</i> Stack before AGORA.	55
<i>Figure 3.30.</i> Stack after AGORA.	55
<i>Figure 3.3.</i> Amplitude spectrum for shot 1004 before and after AGORA.	56
<i>Figure 3.32.a.</i> Shot 1004 After AGORA.	57
<i>Figure 3.32.b.</i> Shot 1004 after the application of (f, k) filter.	57
<i>Figure 3.33.a.</i> The stack of the profile 16NG04 after the application of (f, k) filter.	58
<i>Figure 3.33.b.</i> Stack of the profile 16NG04 after AGORA.	59
<i>Figure 3.34.</i> Amplitude spectra of shot 1004, after (f, k) filtering and after AGORA.	59
<i>Figure 3.35.</i> Amplitude spectra of the raw shot 1004, after (f, k) filtering and after AGORA.	60







## LIST OF TABLES

<b>N°</b>	<b>Title</b>	<b>Page</b>
Table 2.1	Sampling in time and space	24
Table 3.1	Tested parameters	47
Table 3.2	tested Parameters for AGORA.	53



***Acknowledgments******Dedications******List of figures******Abstract******Introduction***<sup>1</sup>***Chapter one: Seismic acquisition and processing generalities***

Introduction.....	3
1.1. Description of seismic signals acquisition. ....	3
1.1.1. Sources.....	3
1.1.2. Sweep.....	3
1.1.3. Seismic Detectors .....	4
1.1.4. Recording Unit .....	4
1.2. Process of correlation in the vibroseis.....	5
1.3. Seismic Recording.....	6
1.4. Seismic signal.....	7
1.4.1. Definition.....	7
1.4.2. Types of wave.....	7
a. Body waves.....	7
a.1. Primary waves.....	7
a.2. Secondary waves.....	7
b. Surface waves.....	8
b.1. Love waves.....	8
b.2. Rayleigh waves.....	8
b.3. Pseudo Rayleigh waves.....	9
1.4.3. Wave's paths.....	10
1.4.4. Seismic reflection.....	10
a. Reflection wave.....	10
b. Concept of acoustic impedance.....	10
c. Reflection coefficient.....	10
1.4.5. Attenuation Phenomena.....	11
1.5. Time space graph t(x).....	11
1.5.1. Reflected arrival.....	11
1.5.2. Linear arrival.....	12

<b>1.6. Noise in seismic acquisition.....</b>	<b>12</b>
<b>1.6.1. Random noise.....</b>	<b>12</b>
<b>a.Ambient noises.....</b>	<b>13</b>
<b>b.Equipment noises.....</b>	<b>13</b>
<b>1.6.2 Organized noises.....</b>	<b>13</b>
<b>a. The diffractions.....</b>	<b>13</b>
<b>b. The refractions.....</b>	<b>13</b>
<b>c.The multiple reflections.....</b>	<b>14</b>
<b>c.1.Short-path multiple.....</b>	<b>15</b>
<b>c.2. Long-path multiple.....</b>	<b>15</b>
<b>c.3. Peg-leg multiple.....</b>	<b>15</b>
<b>1.7. Seismic data processing.....</b>	<b>15</b>
<b>1.7.1. Elevation statics.....</b>	<b>16</b>
<b>1.7.2.Near-surface velocity anomalies.....</b>	<b>16</b>
<b>1.7.3. Normal move-out(NMO).....</b>	<b>17</b>
<b>1.7.3.1.NMO procedure.....</b>	<b>18</b>
<b>1.7.4. Migration.....</b>	<b>20</b>
<b>1.8. Summary.....</b>	<b>21</b>
<b><i>Chapter two: <math>(f, k)</math> and AGORA filters</i></b>	
<b>Introduction.....</b>	<b>22</b>
<b>2.1. Time and spatial sampling of a continuous function.....</b>	<b>22</b>
<b>2.1.1. Aliasing in time.....</b>	<b>23</b>
<b>2.1.2. Aliasing in the direction of wave number.....</b>	<b>23</b>
<b>2.2.(f, k) filter.....</b>	<b>24</b>
<b>2.2.1. Definition.....</b>	<b>24</b>
<b>2.2.2.Signal and noise presentation in the plan (f, k).....</b>	<b>26</b>
<b>2.2.3. (f, k) filter procedure.....</b>	<b>27</b>
<b>2.3. AGORA modeling.....</b>	<b>28</b>
<b>2.3.1. Technical background.....</b>	<b>28</b>
<b>2.4. Summary.....</b>	<b>33</b>
<b><i>Chapter three: Application on real seismic data</i></b>	
<b>Introduction.....</b>	<b>34</b>
<b>3.1. Geological framework of the region.....</b>	<b>34</b>
<b>3.2. Description of the study profile.....</b>	<b>35</b>

3.3. Acquisition parameters.....	36
3.3.1. Recording parameters.....	36
3.3.2. Source parameters.....	36
3.3.3. Receiving parameters.....	36
3.4. random noise Attenuation.....	37
3.4.1 Trace editing.....	37
3.4.1.1. Result Analysis and comparison.....	38
3.4.2. Despiking.....	41
3.4.2.1. Results Analysis and comparison.....	42
3.5. Ground rolls attenuations.....	45
3.5.1 Attenuation by (f, k) filter.....	47
3.5.1.1. Discussion and results.....	48
3.5.2. Ground roll Attenuation using AGORA.....	53
3.5.2.1. Results comments and Analyses.....	53
3.6.3 Comparison between the two methods.....	57
3.7. Summary.....	60
<b>Conclusion and further work.....</b>	<b>61</b>

## ***Bibliography***

## ***Appendices***





## ACKNOWLEDGMENTS

*We express our deepest gratitude to our supervisor, Dr. Dalila CHERIFI, who offered invaluable assistance, support and guidance. Without her we would never have been able to say what is about to follow. We hold to thank Mr.Farid CHEGROUCHE, and Mr. Youcef LAADJAJ heads of Department at “EN.A.GEO” «Enterprise National Algérien de Géophysique» for all help he provided for us.*

*We thank all the teachers, the library and security staff along the five years of studies and also those who helped us to prepare this modest investigation by encouragement or by advice.*

*We would also like to thank Mr.lyasBOUCHAOUI for his considerable help.*

*Mr. President and the members of jury find here the expression of our sharp gratitude and our respect for the honor that they make us while agreeing to examine this work.*

*We would especially thank our families for their constant support and encouragement.*

# ***Dedication***

*To the greatest woman I've ever worked with "Dalila CHERIFI"*

*To my mother, and my father who made me the man I am today*

*To my young sister Dounia, and my brother Anis*

*To my lovely aunt, Both uncles Abderahmane and Sofiane, and all my family  
faithfully*

*To my roommates and partners, Ramzi, Yassine, Ameer, Lokmane, Sidali, and  
all my friends who were by my side during good, and bad times.*

*Salah.*

*To the best teacher in the world and the greatest woman I have ever met  
"Dalila Cherifi"*

*To my lovely mother, and my great father*

*To my brothers and sisters*

*To my grandfather and grandmother "yemma"*

*To my uncle Houcine Badouchi, I really appreciate your support and help, and  
all my family faithfully*

*To my partner Salah Nekhoul*

*To my business partner "Ameer Soualmi", we will be a rich some day*

*To my roommates and partners, Ameer, Ramzi, and all my friends who were by  
my side during good, and bad times.*

*To my brother Alla Elldine Hedib, I wish for you all the success*

*To my cousins Milano, Hmimed, Sidali, Islam*

*To all my social media friends and fans*

*Yassine*



## ABSTRACT

The seismic method is the most used method to capture and study the subsurface. The discipline of subsurface seismic imaging, or mapping the subsurface using seismic waves, takes a remote sensing approach to probe the Earth's interior. The seismic method goes over three major phases: data acquisition, processing, and the interpretation processes. During the process of the acquisition and the transmission, the data is often corrupted by the different types of noises.

Throughout our work, we focused on the study of the two dimensions' filters ( $f, k$ ) and AGORA. The objective of the study was to attenuate coherent dispersive ground roll energy and to establish which of the techniques would attenuate the ground rolls most effectively. Both filters ( $f, k$ ) and AGORA use the Forward Fourier Transform and modeling in the  $(F, X)$  domain to provide an appropriate plan for separating the noisy signal from the useful signal in this new domains. We have applied the two previous filters on the real data and we compared their effects.

However, AGORA was a better technique than the  $f-k$  for noise attenuation based on the clarity of primary events which we seek to enhance at the expense of the ground roll energy.

## Introduction

The oil and gas industry uses 2D seismic, or seismic reflection, to analyze the structure of the rocks hidden beneath the surface. Seismic reflection involves sending acoustic energy into the ground (using an energy source such as a Vibroseis) to create a sound picture beneath the surface. Each stratigraphic layer within the Earth reflects a portion of the energy back and allows the rest to pass through. These reflected energy waves are recorded by sensitive receivers, or geophones, at the surface. Each receiver's reading of the reflected energy waves is recorded onto magnetic tape then the shot location is moved along and the process repeated. Typically, the recorded signals are subjected to further processing before they are ready to be interpreted, an area of significant active research within industry and academia. In general, the more complex the geology of the area under study, the more sophisticated techniques are required to remove noise and increase resolution. Modern seismic reflection surveys contain large amount of data and so require large amounts of computer processing.

The purpose of this thesis is to manipulate the acquired data into an image that can be used to infer the sub-surface structure. Only minimal processing would be required if we had a perfect acquisition system. Processing consists of the application of a series of computer routines to the acquired data guided by the hand of the processing geophysicist. There is no single "correct" processing sequence for a given volume of data. At several stages judgements or interpretations have to be made which are often subjective and rely on the processors experience or bias.

The seismic data is recorded into what is termed the time-offset domain. However, it is affected by the surface waves that mask the primary reflections. They are considered as a low frequency noise with very high amplitudes. The processing sequence makes it possible to filter these recordings. Many techniques are used for this purpose, among these techniques the  $(f, k)$  filter and AGORA modeling.

This project aims at eliminating the noise from seismic data using the above two filters.

This report is organized then in the following way:

- The first chapter gives a general overview about our topic which consists on Ground-roll noise filtering of seismic petroleum data. The chapter is devoted

for some generalities about seismic data acquisition and basic seismic data processing. The second chapter is about the theoretical part where we explain all the theories related to the two filters used.

- The third chapter includes the application of the two filters on thereal data.
- Finally, we end up with a conclusion by presenting the performances, the limits of our approach and suggestions for further work.

“The application part is achieved during our training period at “E.NA.GEO” (Entreprise Nationale de Géophysique), Boumerdes.”

## Introduction

Seismic method consists of generating very low-amplitude artificial earthquakes at predetermined times and positions. The induced seismic disturbances are recorded by receiver spreads made up of traces. An energy source made up of one or more source elements generates the seismic disturbance.

This chapter is devoted to the seismic reflection, the information common to wave propagation and the different phenomenon that they undergo in the layers of the subsurface. Also is to give a review of the fundamentals and the current knowledge about seismic noise. The first problem one encounters with seismic noise is the term “seismic noise” itself. After that we will see the basic phases processing in seismic data processing, starting from the static corrections, normal move-out, and the migration.

### 1.1. Description of seismic signals acquisition:

Collecting seismic data requires an energy source to generate waves and sensors to receive those waves. The appropriate energy source and receiver depend on the location and the application. Here, we describe the different types of equipment used for seismic data acquisition.

#### 1.1.1. Sources:

The seismic source on land is usually either dynamite or vibroseis, a vibrating mechanism mounted on large trucks -the most used source in seismic terrestrial- which provides records of high quality as a result of progression seismic land.

#### 1.1.2. Sweep:

It is a significant instantaneous energy emitted by a seismic vibroseis. Its expression is in the form of sinusoidal[1]:

$$s(t) = A(t) \sin \{ \theta(t) \} \quad (1.1)$$

Where:

$A(t)$ : The amplitude of the signal

$t$ : Time of emission

$\theta(t)$ : The phase

### 1.1.3. Seismic Detectors:

The seismic energy generated by each shot is detected and recorded at a variety of distances from the source location by Geophone which is an instrument that transforms a ground vibration, due to the passage of a wave into an electric voltage. The latter is transmitted by the cables to the recording laboratory.

Geophone is composed of a magnet inside a coil suspended with a spring. The principle of its operation is based on Lenz's theorem:  $E = -\frac{\partial \phi}{\partial t}$  (1.2)

Where:

$E$  :Potential difference.

$\phi$ :The flow of the magnetic field.

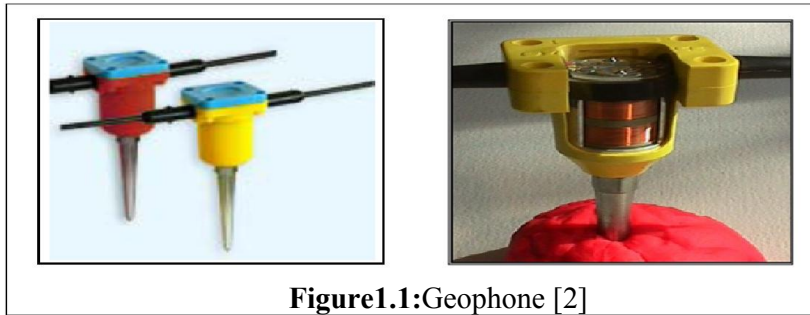


**Figure 1.1:**Geophone [2]

The signal received will follow a path moving through different devices. First, it passes through Field Digitizing Unit (FDU) which converts analogue signals to digital signals. The line voltage provided to the FDUs is supplied through the Link's cables from dedicated field units called LAULs (Line Acquisition Unit Line). The last unit of the acquisition is LAUX (Line Acquisition Unit-Crossing). It is an interface between the line of acquisition and the recording system.

### 1.1.4. Recording Unit:

It is a laboratory where converting all electrical signals provided by the elements of the acquisition system[1]. It consists of a unit called «408UL control module » which aims at the sampling signal with a step of 2ms. Then, the signal is injected inside a correlator to correlate the sweep reference with the received signal. Thus, we obtain the seismic trace which is posted on the screen and is recorded on a magnetic tape.



## 1.2. Process of correlation in the vibroseis:

One important process is the vibroseis correlation. This involves cross correlation of a sweep signal with the recorded vibroseis trace. The seismic trace is the combination of both signal(wanted data) and noise. For every source event, each receiver generates a seismogram or trace, which is a time series representing the earth movement at the receiver location.

The seismic trace is defined as the convolution of an input seismic signal with an earth model composed of discrete reflectors [3].

$$s(t) = e(t) * [r(t) + n(t)] \quad (1.3)$$

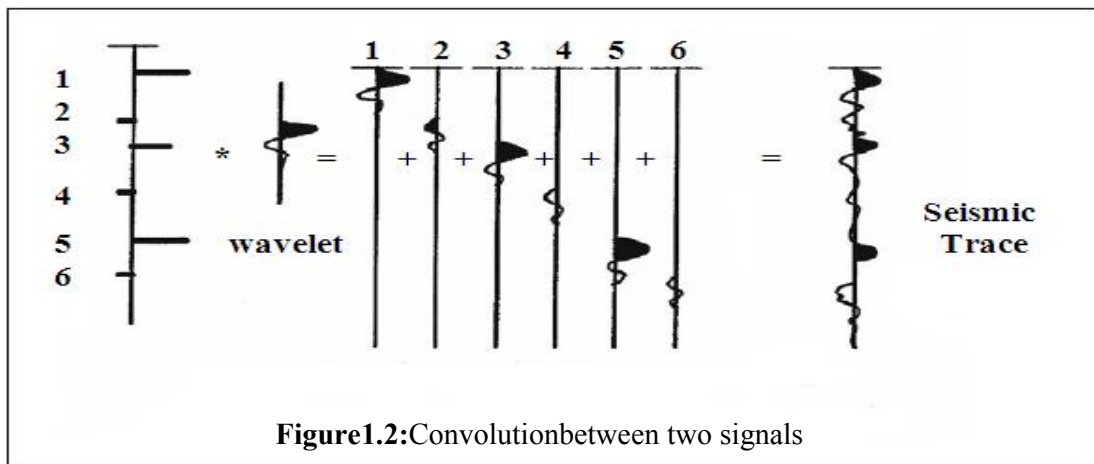
Where:

$s(t)$ : The recorded vibroseis signal

$e(t)$ : The sweep pulse

$r(t)$ : The reflection coefficients

$n(t)$ : Negligible random noise



A vibroseis trace must be processed to produce a replacement trace with a signal equivalent to that of an impulsive source. This is accomplished by cross-correlating the raw seismogram with the vibroseis sweep[3].

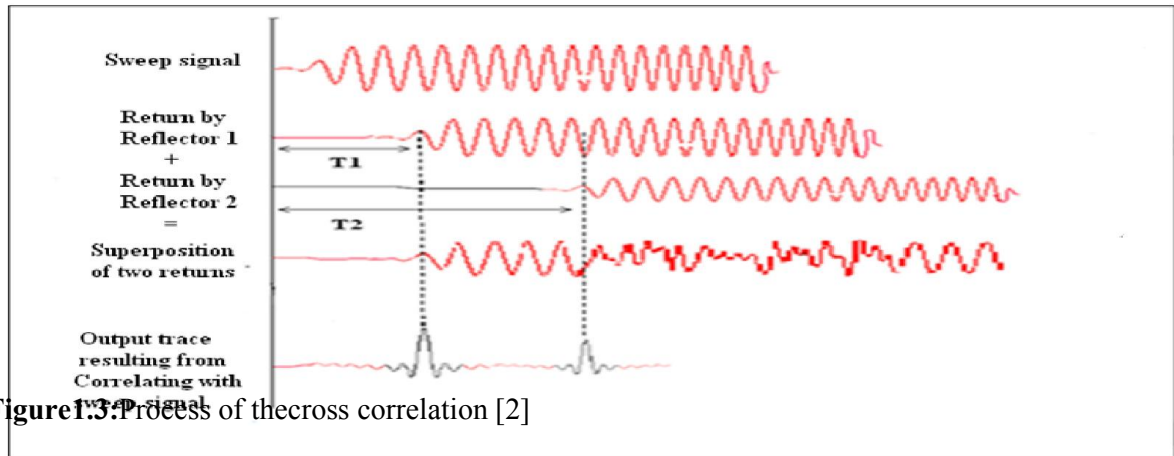


Figure 1.3: Process of the cross correlation [2]

### 1.3. Seismic Recording:

The geometric acquisition is defined by the distribution of the source and receiver groups.

Each trace can be a single sensor, or several sensors forming an array. Therefore, the received signals are recorded on a vertical plan having source-receiver axis. This type of acquisition is called 2D profile

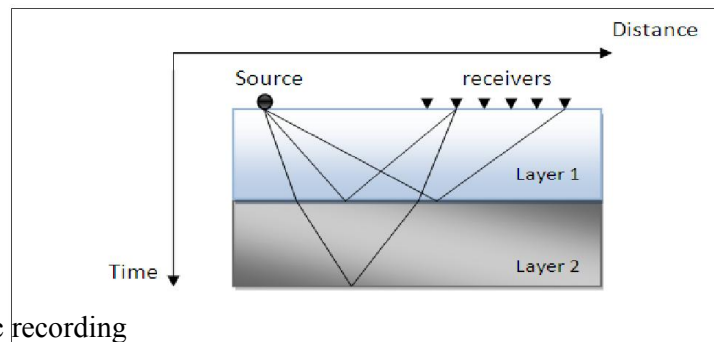
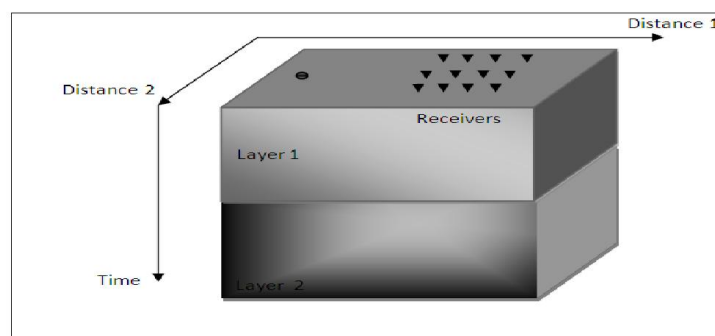


Figure 1.4: 2D seismic recording

For the best reconstitution of the image of the subsurface, we are going to put several lines of antenna, so the recording will depend on a third variable which is the distance between the different trace 2D. Consequently, we obtained a seismic data cube consisting of collection of sections parallel to each other. This type is a 3D acquisition.



**Figure1.5:** 3D seismic recording**1.4. Seismic signal:**

Acquisition of seismic exploration data involves the generation of seismic waves, and their subsequent detection after passing through or reflecting off the region of interest.

**1.4.1. Definition:**

Seismic signal is a mechanical wave which propagates through the Earth under the elastic property. Its principle is[4]:

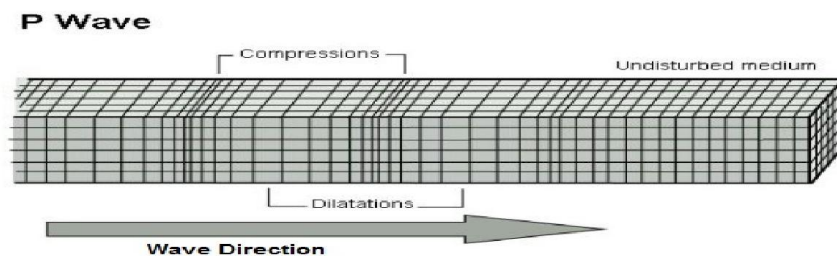
A solid body can be deformed by the application of an external force. If the solid is perfectly elastic, it will return back to its original shape once that force is removed. In the context of exploration seismology, the Earth is generally considered as perfectly elastic because the stresses generated by seismic exploration activities are too small to permanently deform subsurface rocks.

**1.4.2. Types of waves:**

Two categories of seismic waves exist; each category consists of several types which all propagate through the earth with different velocity, amplitude and particle motion[4].

**a. Body waves:** Body waves travel through the interior of the Earth along paths controlled by the material properties in terms of density and modulus (stiffness). Two types of particle motion result in two types of body waves: Primary and Secondary waves.

**a.1. Primary waves:** An elastic body wave or sound wave in which particles oscillate in the direction the wave propagates. The first arriving waves at the recording station, they are the quickest and have a compression particle motion parallel to the direction of travel.

**Figure1.6:**P wave[5]

**a.2. Secondary waves:** An elastic body wave in which particles oscillate perpendicular to the direction in which the wave propagates. S-waves are generated by most land seismic sources. P-waves that impinge on an interface at non-normal incidence can produce S-waves, which in that case are known as converted waves. S-waves can likewise be converted to P-waves. S-waves, or shear waves, travel more slowly than P-waves and cannot travel through fluids because fluids do not support shear.

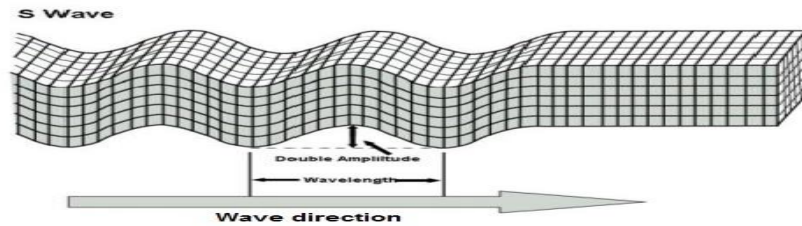


**Figure1.7:**S wave[5]

**b. Surface waves:** The waves that propagate at the interface between two media as opposed to through a medium. The surface waves can travel at the interface between the Earth and air, or the Earth and water. Love waves and Rayleigh waves are surface waves.

**b.1. Love waves:** They are horizontally polarized shear waves (SH waves), existing only in the presence of a semi-infinite medium overlain by an upper layer of finite thickness.[5] They usually travel slightly faster than Rayleigh waves, about 90% of the S wave velocity, and have the largest amplitude.

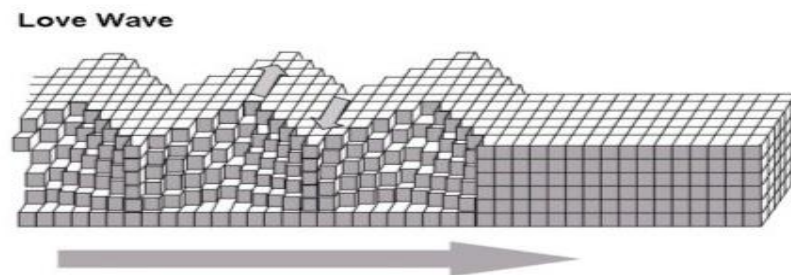


**Figure1.8:**Love wave [5]

**b.2. Rayleigh waves:** A type of surface wave in which particles move in an elliptical path within the vertical plane containing the direction of wave propagation. At the top of the elliptical path, particles travel opposite to the direction of propagation, and at the bottom of the path they travel in the direction of propagation. Because Rayleigh waves are dispersive, with different

wavelengths traveling at different velocities, they are useful in evaluation of velocity variation with depth. Rayleigh waves make up most of the energy recorded as ground roll.

**Rayleigh Wave**

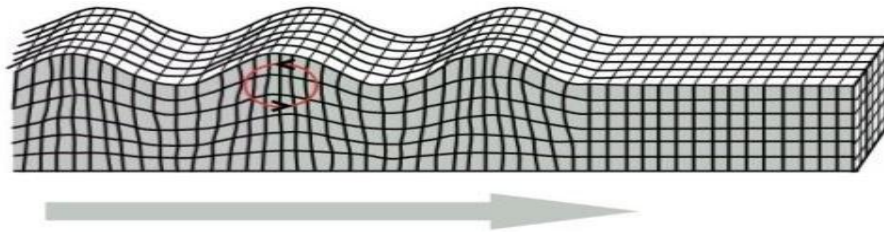


**Figure1.9:** Rayleigh wave [5]

### **b.3. Pseudo Rayleigh waves:**

The presence of the weathered zone modifies Rayleigh wave's characteristics to the pseudo-Rayleigh called ground-roll.

#### **1.4.3. Wave's paths:**

Seismic wave behaviour can be understood in terms of ray path theory[4].

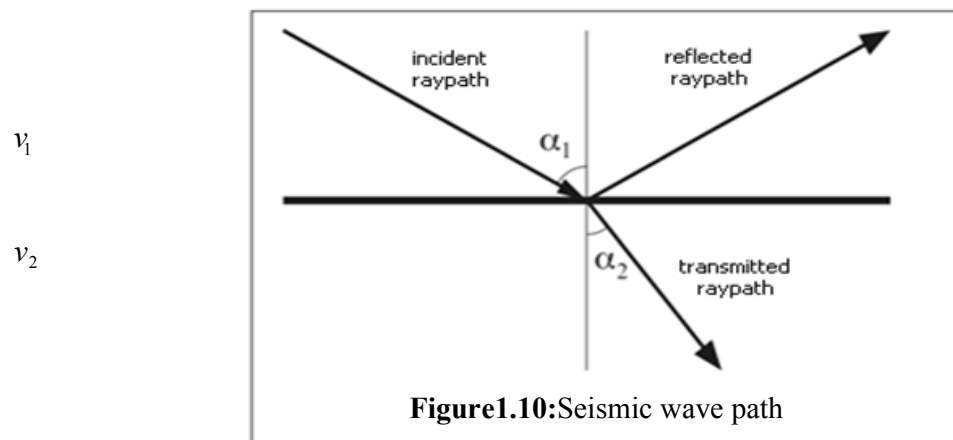


**Figure1.10:** Seismic wave path

Figure (2.9) shows a two-layer model with a higher velocity layer over a lower velocity layer. In the figure, a down-going ray in the upper layer is partitioned into an up-going reflected ray and a down-going transmitted ray at the layer boundary.

The transmission angle can be calculated using Snell's law, which is given by:

$$\frac{\sin \alpha_1}{v_1} = \frac{\sin \alpha_2}{v_2} \quad (1.5)$$

Where  $v_1$  and  $v_2$  are velocities in the upper and lower layers,  $\alpha_1$  is the angle of the incident ray path with respect to the vertical, and  $\alpha_2$  is the angle of the transmitted ray path with respect to the vertical.

#### 1.4.4. Seismic reflection[4]:

The most frequently practiced form of seismic acquisition is the reflection seismic survey.

The acquisition and processing of reflection seismic data usually result in a seismic image of impedance interfaces. These are assumed to follow lithologic boundaries, and then the seismic image is actually an image of subsurface geological units and the structures they form. The seismic reflection deal with body waves since they carry the information.

##### a. Reflection wave:

During the wave propagation in the various layers of the ground, they undergo reflections due to the changes of the parameters characteristics of the propagation medium such as the impedance. The point of reflection is called mirror point, the medium point is the point located between the point of shot and the receiving trace.

These reflection waves are used and studied because they have several effects to know:

- They make it possible to define all the interfaces whatever is their nature.
- They give an image very close to the geological reality of the subsurface.
- They enable us to work in the zones with dip.
- They have a focusing device, i.e. they do not need to slacken the device of measurement to increase their depths of investigation.

##### b. Concept of acoustic impedance:

Wave velocity  $v$  and density  $\rho$  are the two main parameters which determine the nature of seismic wave propagation, their product  $z$  known as the acoustic impedance.

$$z = v\rho \quad (1.6)$$

##### c. Reflection coefficient:

It is the ratio between the amplitude of the reflected wave and the transmitted wave. The relation between the reflection coefficient and the impedance is[6]:

$$r = \frac{v_1\rho_1 - v_2\rho_2}{v_1\rho_1 + v_2\rho_2} \quad (1.7)$$

Where:

$v_i$ : Velocity of propagation in the medium  $i$ .

$\rho_i$ : Density of the medium.

#### 1.4.5. Attenuation Phenomena:

Seismic waves are reduced in amplitude as they are propagated through the earth due to three factors[6]:

- Geometrical divergence: at large distances from the source spherical waves reduce in amplitude, and they are proportional to the distance( $1/x$ ).

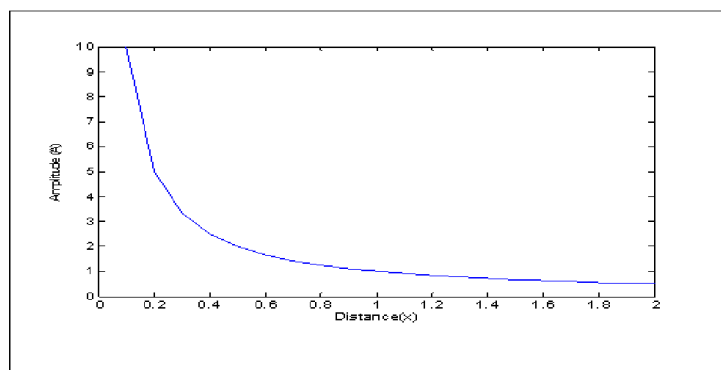


**Figure1.11:**Geometrical Divergence

- Partial transmission and reflection at acoustic boundaries.
- Absorption of energy in the medium of transmission.

### 1.5. Time space graph $t(x)$ :

#### 1.5.1. Reflected arrival:

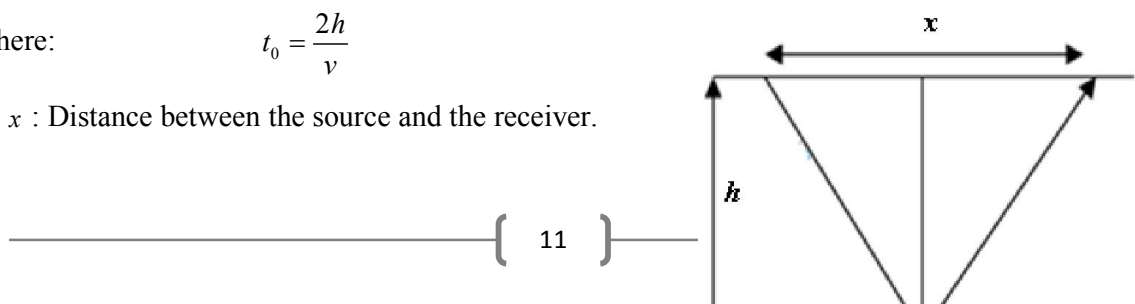
The time travel of the signal from the source to the receiver passing by depth point is given by the following equation [6]:

$$t(x) = \frac{2}{v} \sqrt{\frac{x^2}{4} + h^2}$$

$$t^2(x) = \frac{x^2}{v^2} + t_0^2 \quad (1.8)$$

Where:  $t_0 = \frac{2h}{v}$

$x$  : Distance between the source and the receiver.



$h$  : The depth.

$t_0$  : Time of intercepts.

$v$  : Velocity of the medium.

**1.5.2. Linear arrival:** is a direct arriving to the detector.

$$t(x) = \frac{x}{v} + t_0 \quad (1.9)$$

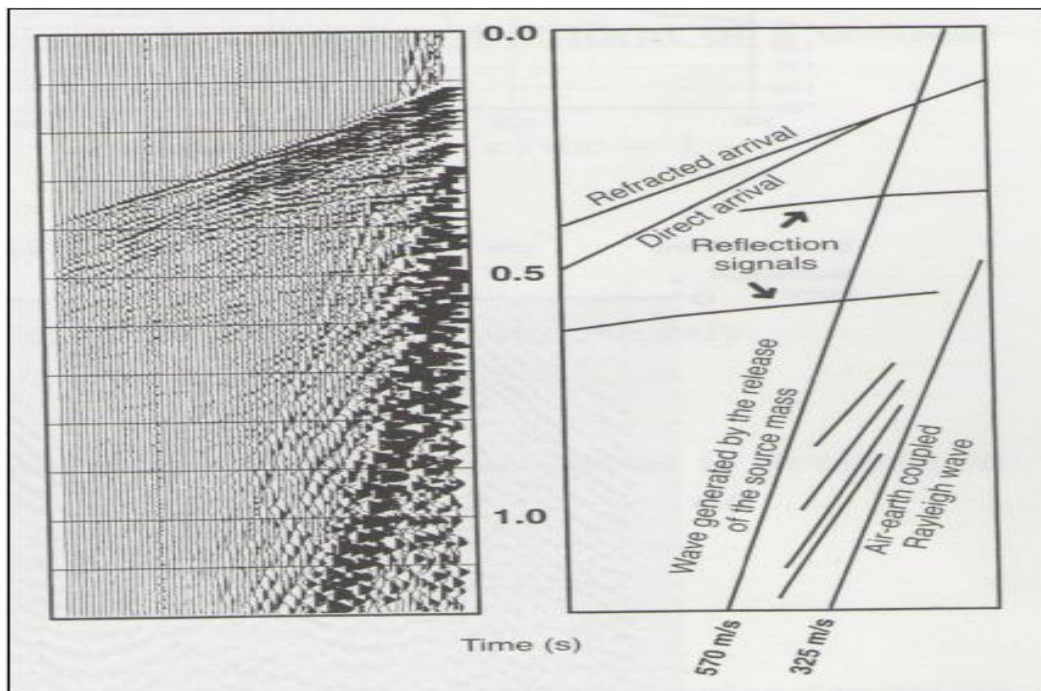


**Figure 1.1:** The different waves in seismic recording[7]

## 1.6. Noise in seismic acquisition:

We distinguish two categories:

### 1.6.1 Random noise:

The random noises are not observed directly and cannot be modeled mathematically. Their effects are noted by jamming of information, for example the seismic horizons become vague and chopped. In practice, a noise with these characteristics does not exist. When recording, the bandwidth of the signal is always limited towards the low frequencies by the cutoff frequency of



---

the geophone (the order of 8 to 10 Hz) and towards the high frequencies by the cut-off frequency of the anti-noise filter. Among these noises, we meet mainly:

**a.Ambient noises:**

These noises are caused by the movement of the soil in the immediate vicinity of a trace. These noises have various origins: movement of people, vehicles, herds, winds ...etc. These noises vary from one trace to another, and have significant energy levels.

**b.Equipment noises:**

All the different types of equipment used in seismic contain noises. Once these noises are determined it's essential to demand the standards necessary for its integral preservation.

**1.6.2Organized noises:**

Conversely to the preceding ones, a noise is said to be organized if it presents a coherence in the domain  $(t, x)$  that is the case of multiple reflections, diffractions, refractions, surface noises ... etc. These noises are characterized by certain physical parameters such as: apparent speed (VA) and frequency (f). An organized noise obeys a law that facilitates its prediction. In our study we will be interested in elimination of the coherent noises (ground-roll), and the multiples. Among these noises we distinguish mainly:

**a. The diffractions:**

The diffracted waves contain valuable information about the structure and composition of the media that generated them. In standard seismic data processing, however diffracted waves are often regarded as noise and are suppressed. Many processing tools are biased against diffractions, whereas intentional suppression may be needed to reduce artifacts or to increase coherency[8].

**b. The refractions:**

In seismic, refractions are always considered as organized noises. They mask the signals by compromising their exploitation. Refracted arrivals have relatively low frequencies and include

several periods. At the processing, the attenuation of these noises is effected by the use of the mute of the first arrivals (reset) of the refracted wave as well as the filtering in frequency and wave number ( $f$ ,  $k$ ) and the summation (multiple coverage) are the means by simple used to remove them. The particular case of these refractions, called reflected refractions, remains delicate to treat.

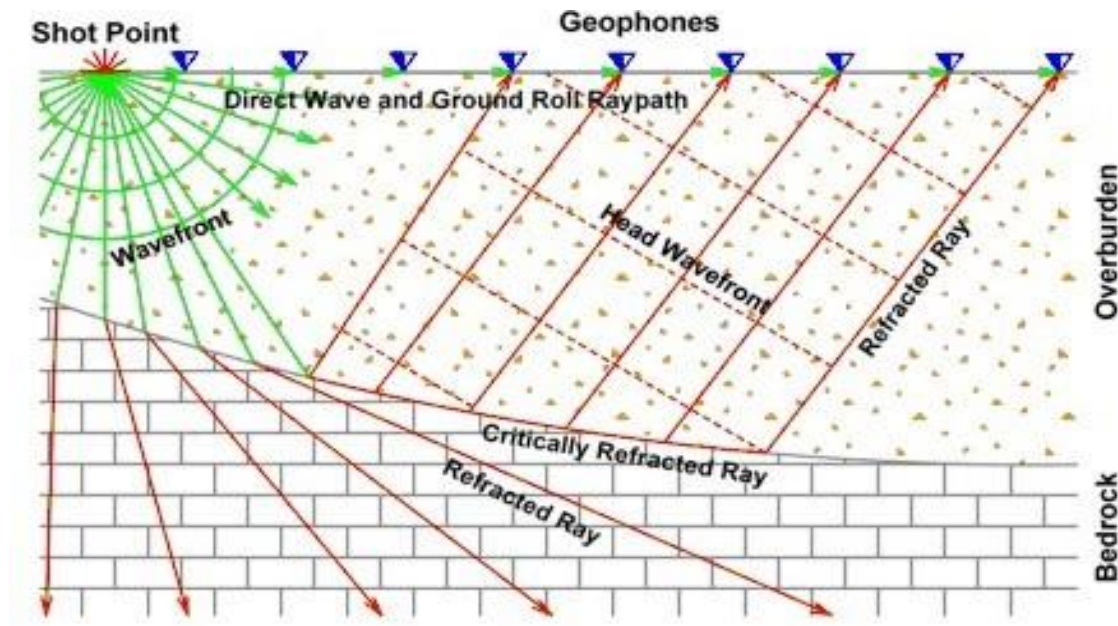


**Figure1.13:**Seismic Refraction geometry[9]

### c.The multiple reflections [10]:

Multiply reflected seismic energy, or any event in seismic data that has incurred more than one reflection in its travel path. There are three types of multiples: long path multiple, short path multiple, and peg-leg multiple.

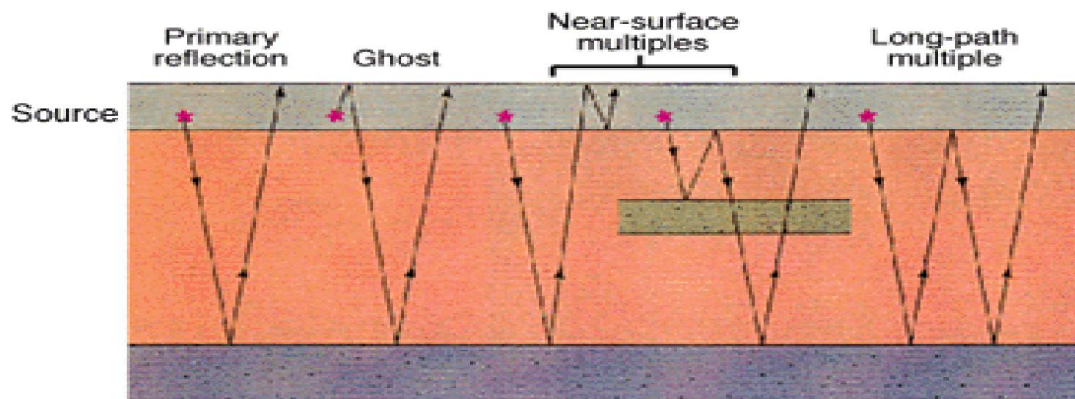


**Figure 2.14:** Seismic multiple reflection [10]

**c.1. Short-path multiple:** Multiply-reflected seismic energy with a shorter travel path than long-path multiples.

**c.2. Long-path multiple:** A type of multiply-reflected seismic energy that appears as an event. Long-path multiples generate distinct events because their travel path is much longer than primary reflections giving rise to them. They typically can be removed by seismic processing.

**c.3. Peg-leg multiple:** A type of short-path multiple, or multiply reflected seismic energy, having an asymmetric path. Short-path multiples are added to primary reflections, tend to come from shallow subsurface phenomena and highly cyclical deposition.

### 1.7. Seismic data processing:

The ideal goal of seismic processing is to have a section which consists of true reflections which arise from structure directly beneath the source. The image should provide quantitative information about geologic structure. Therefore correcting near-surface velocity and elevation variations with statics is an essential step and static corrections are very important in the processing of land data, which can improve the qualities of subsequent processing steps and are related to the quality and resolution of final imaged section. Static corrections are defined as: corrections applied to seismic data to compensate for the effects of variations in elevation, weathering thickness, weathering velocity, or reference to a datum. The objective is to determine the reflection arrival times which would have been observed if all measurements had been made on a (usually) flat plane with no weathering or low-velocity material present. There are many

issues which are associated with the near surface and related with the variations of velocity and thickness in the near-surface layers[11].

So before carrying out the normal move-out(NMO) correction it is usually necessary to perform a static correction, which amounts to moving the entire seismic trace up or down in time.

In this part we will be introducing three main steps in seismic data processing, which are: Static corrections, normal move-out(NMO), and the migration.

### 1.7.1. Elevation statics :

The correction procedure involves establishing a datum on which to locate source and receiver, and then adding or subtracting the incremental time. The reference velocity will be that of the upper layer.

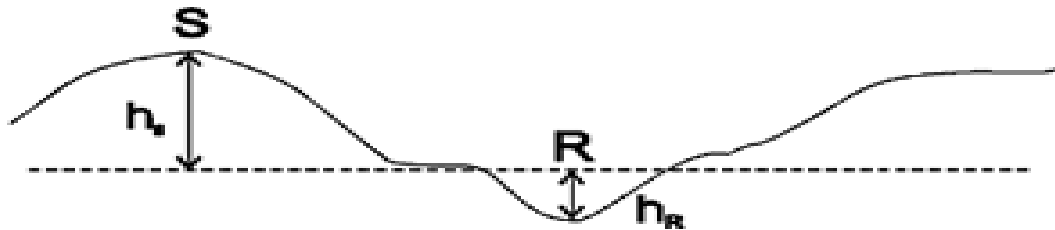


Figure 1.15.Static correction[12]

The reflections of interest are usually coming from great depth and the upcoming energy is traveling nearly vertical. So the static correction due to elevation expressed as a change in travel time is:

$$\Delta t = \frac{h_s}{v_1} - \frac{h_r}{v_1} \quad (1.10)$$

And is subtracted from the record. That's the whole seismic record is shifted in time by the value  $\Delta t$ .

### 1.7.2.Near-surface velocity anomalies :

We may also have some shifts in time if there is anomalous velocity beneath a source or receiver or if the thickness of the weathering layer changes. The amount to be subtracted from the seismic trace time is given by the following formula:

$$\Delta t = \frac{h_a}{v_a} - \frac{h_a}{v_1} \quad (1.11)$$

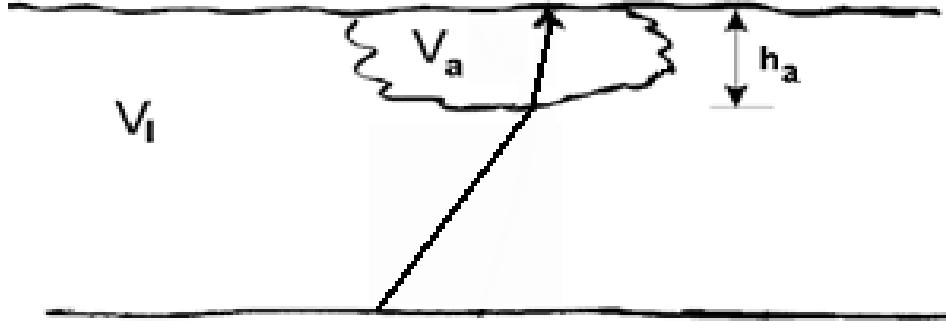


**Figure 1.16:** Near-surface[12]

After static correction, the subsurface events will look more like an hyperbola and they will be ready for velocity analysis, NMO and stacking.

### 1.7.3. Normal move-out(NMO): Stacking data in CMP gathers

The conventional NMO hyperbola has its roots in the early 1960s, and it is still used widely in seismic exploration. For a planar horizontal reflector with homogeneous, it provides exact travel-times, and for dominantly horizontal layering, often encountered in sedimentary environments, it is likewise known to lead to accurate multi coverage reflection travel-time estimates[12].

The travel time curve of the reflections for different offset between source and receiver is calculated using :

$$t^2 = t_0^2 + \frac{x^2}{v_{stack}^2} \quad (1.12)$$

For this formula the NMO correction can be derived and given by :

$$\Delta t = t_0 - t(x) \text{ with } t(x) = \sqrt{t_0^2 + \frac{x^2}{v_{stack}^2}} \quad (1.13)$$

The Move-out  $\Delta t$  is the difference in traveltimes for a receiver at a distance  $x$  from the source and the travel time  $t_0$  for zero-offset distance.

Principle:

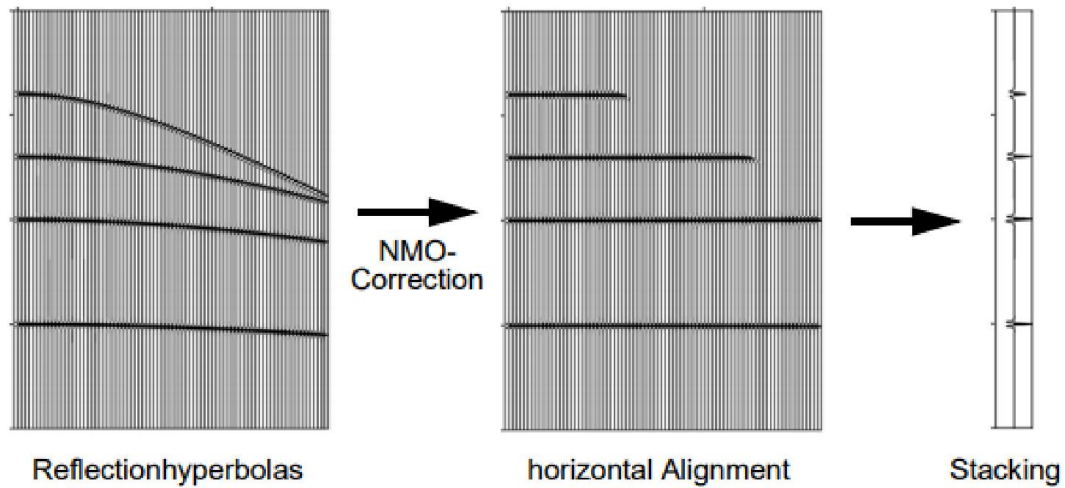


Figure 1.17: Normal move-out correction [13]

### 1.7.3.1. NMO procedure [12] :

The travel time curve from the reflector will appear approximately as a hyperbola. Unlike for the common shot gather, in the CMP gather all of the arrivals correspond to the same reflection point.

The hyperbolic representation for the travel time curve is exact if the velocity above the reflector is constant, and if the reflector is flat. For layered media we saw that the travel time curve was hyperbolic, but the velocity used should be the RMS velocity. Unfortunately, we don't know what this velocity is, so we attempt to estimate it from the data themselves. We proceed as follows:

1. We assume that each reflection event in a CMP gather has a travel time that corresponds to a hyperbola,

$$t^2 = t_0^2 + \frac{x^2}{v_{stack}^2} \quad (1.12)$$

Where  $V_{stack}$  is called the stacking velocity.

2. For each reflection event hyperbola, we perform a velocity analysis to find  $V_{stack}$ . This is done by first choosing  $t_0$ . Then we choose a trial value of velocity  $V_1$ . The associated travel time hyperbola is generated and it forms a trajectory on the CMP gather. We sum the energy of the seismic traces along the trajectory and plot this value on a graph of velocity versus energy. Repeat this procedure for different trial velocities. Choose as the  $V_{stack}$  velocity that yields the largest energy. In the diagram below  $V_2$  represents the stacking velocity. The term cross power can be interpreted as total energy.

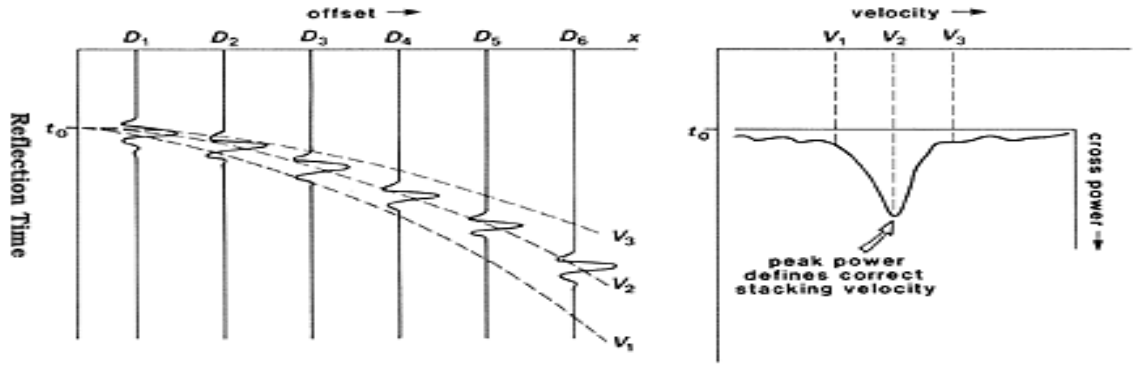


**Figure 1.18:**reflection event hyperbola[12]

3. We calculate the Normal Move-out Correction: Again, using the hyperbola corresponding to  $V_{stack}$ , compute the normal move-out for each trace and then adjust the reflection time by the amount  $\Delta t$ .

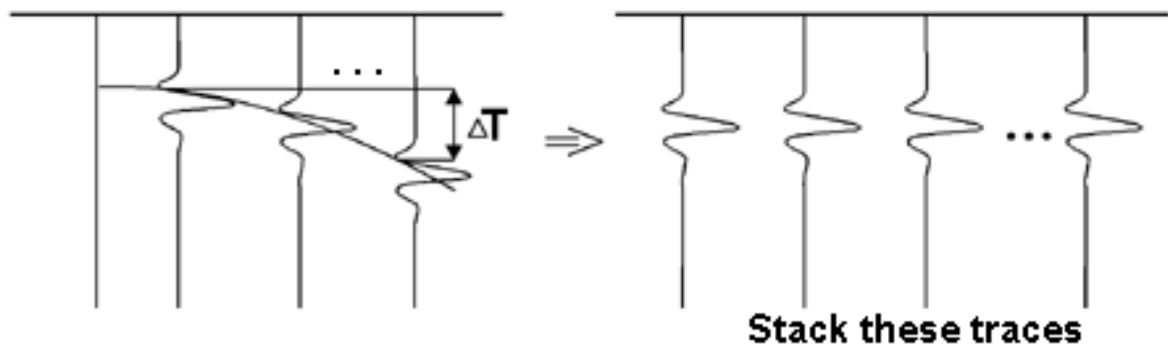


**Figure 1.19:** NMO correction, stacked traces [12]

4. Finally, stacking the normal move-out corrected traces generates a single trace. Each trace corresponds to a zero-offset trace, that is, the seismic trace that would have been recorded by a receiver that is coincident with the source.

#### 1.7.4. Migration:

A processing step which is important in putting reflectors in their correct location is migration. The need for migration is most evident when layers are not flat lying. Consider a single dipping layer and seismic traces corresponding to a coincident source and receiver.

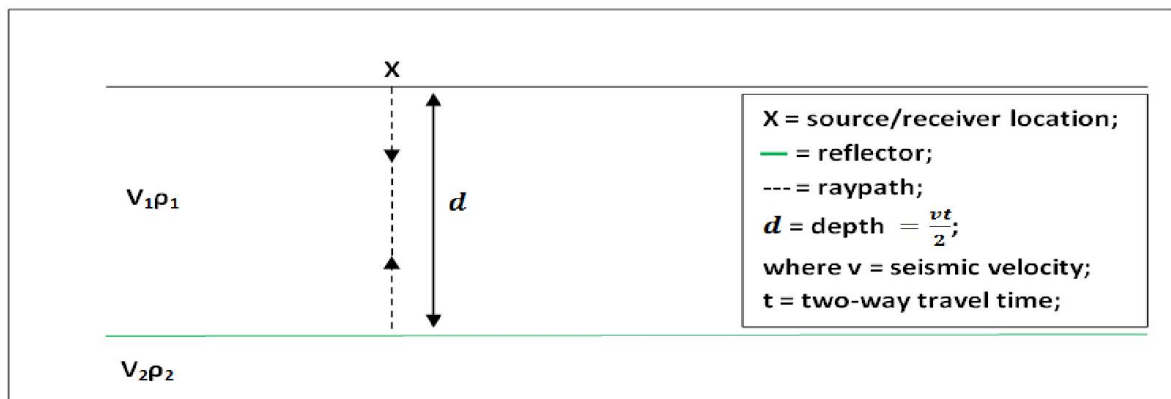


**Figure 1.20:** Diagram showing the ray path for a zero-offset reflection from a horizontal reflector [13]

The reflection time is given by  $t = \frac{2d}{v}$



But when we plot the section we think of the reflections arriving from directly beneath the shot. The result is that a sloping reflector in the ground will appear as a sloping reflector in the seismic section, but the slopes will be different. The true dip will be greater than that observed on the section. The relationship between the two dips is

$$\sin(\alpha_t) = \tan(\alpha_s) \quad (1.14)$$

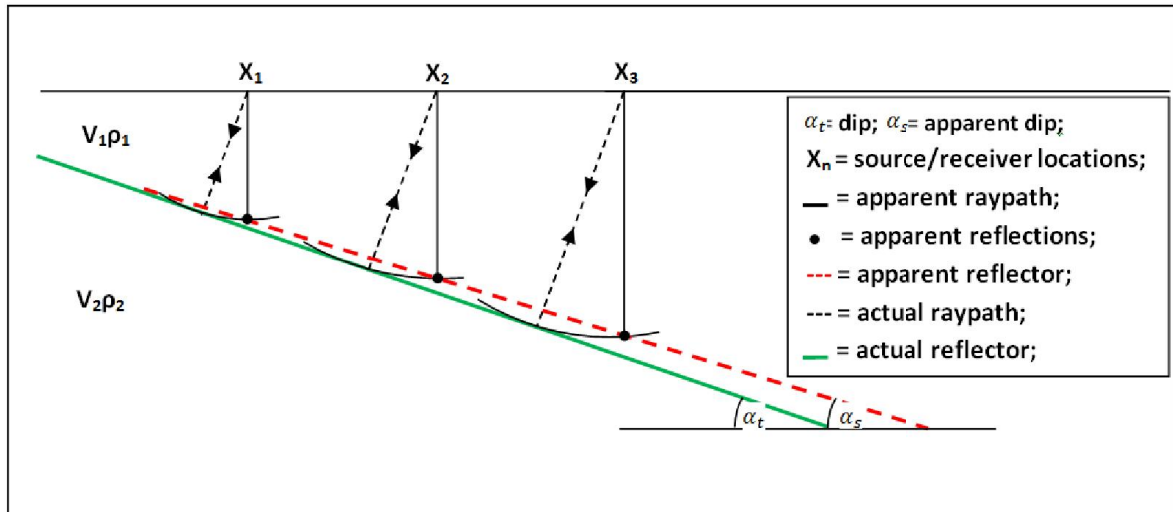


**Figure 1.21:**Diagram showing the ray path for a zero-offset reflection from a dipping reflector and the resultant apparent dip [13]

### 1.8. Summary:

In this chapter we have seen that the seismic acquisition enables us to get information and the data that's needed later in the processing. We have seen also the different types of noises that we always face in seismic processing. There many steps that we pass over in the processing of the information, and they all tend to enhance the quality of the image. Even though these data are rough and are not interpretable, and here where it comes the necessity of the filtering where we are going to deeply discuss it later in the next chapter.

## Introduction

The seismic traces generated by the same seismic disturbance make up a seismic record represented in  $(x, t)$  plan, which is sampled, digitized, and then recorded on magnetic media.

These records are contaminated with strong coherent noise such as ground-roll that overwhelms the subsurface reflections. Therefore, the  $(f, k)$  and AGORA filters are developed to reduce the effects of the ground-roll in the seismic records. The  $(f, k)$  method is based on the possibility of separating the signal and noise based on their distinguishing characteristics such as frequency content. Same thing for AGORA, this approach uses the ground-roll characteristics contained in each shot (group and phase velocities) to perform an Elastic Modeling of the “signal” and “noise (Surface Waves)” in the FX domain for several frequency bands. After that, the least squares approach is used to adapt the “noise” to the input data before subtracting it. This part has an objective of studying the theorems and procedures of these filters.

### 2.1. Time and spatial sampling of a continuous function:

The seismic data are data sampled in time and distance. The correct application of sampling is a key of reconstruction the image of the subsurface. Sampling is achieved through the mechanism of the Dirac delta function. The sampling steps in time and space are denoted  $\Delta_t$  and  $\Delta_x$  respectively. The continuous function  $s(x, t)$  is that [14]:

$$g(i\Delta_x, j\Delta_t) = s(x, t) \cdot \delta(x - i\Delta_x, t - j\Delta_t) \quad (2.1)$$

The sampled seismic function is then written [7]:

$$g(x, t) = \sum_{i=1}^N \sum_{j=1}^M g(i\Delta_x, j\Delta_t) = s(x, t) \sum_{i=1}^N \sum_{j=1}^M \delta(x - i\Delta_x, t - j\Delta_t) \quad (2.2)$$

Where:

N is the number of traces (in space).

M is the number of time samples.

The frequency domain (appendix B) function is written:

$$G(k, f) = S(k, f) * \sum_{l=-\infty}^{+\infty} \sum_{p=-\infty}^{+\infty} \delta(k - \frac{l}{\Delta_x}, f - \frac{p}{\Delta_t}) \quad (2.3)$$

The spectrum of the continuous function repeats every  $1/\Delta_x$  in wavenumber  $k$  and every  $1/\Delta_t$  in frequency  $f$ . If the spectrum of the continuous function is not zero outside of the range:

$$\left[ -\frac{1}{2\Delta_t}, +\frac{1}{2\Delta_t} \right], \left[ -\frac{1}{2\Delta_x}, +\frac{1}{2\Delta_x} \right].$$

The spectra are superimposed at the repetition points, the phenomenon being called aliasing.

### 2.1.1. Aliasing in time:

To avoid the aliasing effect it is necessary to filter the continuous function in  $f$  before sampling, to remove those frequencies higher than Nyquist (or Shannon) frequency  $F_N = 1/2\Delta_t$  ( $f_{\max} \leq 1/2\Delta_t$ ).

The Nyquist frequency is the one that the amplitude of the spectrum is zero.

$\Delta_t$  : Sampling interval.

$f_{\max}$  : Maximum frequency in the signal.

In seismic onshore, the signal is sampled in the laboratory with a step  $\Delta_t$  of 2ms, so the Nyquist frequency is 250 Hz[1]. Temporal anti-alias filtering is designed to reduce the seismic energy to a negligible level beyond  $F_N$ .

### 2.1.2. Aliasing in the direction of wave number:

To avoid this effect it is essentially to filter the continuous function in wave numbers higher than the Nyquist wave number  $K_N = 1/2\Delta_x$  that means  $\left(k_{\max} \leq 1/2\Delta_x\right)$ .

Spatial anti-alias filtering is implemented by means of arrays composed of  $N$  sensors with separation  $e$ . The interval  $e$  is small and chosen so that the seismic function has no energy beyond[1]:

$$k_{Ne} = 1/2e \quad (2.4)$$

Array filtering or multi-geophone filtering assures the attenuation of wave numbers higher than

$$\frac{1}{Ne} = \frac{1}{2\Delta_x}$$

Where:  $\Delta_x$  is the sampling interval corresponding to the Nyquist wave number  $1/Ne$

$k_{\max}$  : Maximum wave number of the signal.

The following box summarizes the effects of sampling[7]:

**Table2.1:** Sampling in time and space

Temporal sampling in $t$	Spatial sampling in $x$
<p>If <math>\Delta_t</math> is the required sampling interval:</p> <p><b>Solution</b></p> <p>Filter the continuous function before sampling to attenuate the amplitude spectrum for</p> $f \geq F_N$ $F_N = \frac{1}{2\Delta_t}$ <p>This filtering is implemented in the recording instruments by analog-anti alias filters.</p>	<p>If <math>\Delta_x</math> is the required sampling interval:</p> <p><b>Problem</b></p> <p>There is no access to the continuous function in <math>x</math></p> <p><b>Solution</b></p> <ol style="list-style-type: none"> <li>1. Sample the function in <math>x</math> at a very small interval <math>e</math> such that there is no energy in the amplitude spectrum beyond <math>k &gt; K_{Ne}</math>.</li> </ol> <p>The Nyquist wave number <math>K_{Ne} = 1/2e</math></p> <ol style="list-style-type: none"> <li>2. Filter the function sampled at interval <math>e</math> to zero the spectrum for <math>K_{Nx} = 1/2\Delta_x</math>.</li> <li>3. For a linear array of <math>N</math> detectors:  <math display="block">K_{Nx} = 1/2\Delta_x = 1/Ne</math> </li> </ol>

## 2.2(f, k) filter:

In time-distance domain the signal and noises are superposed and they are difficult to remove. The (f,k) method is based on the possibility of separating the signal and noise based on their distinguishing characteristics such as frequency content. One solution is to change the representation of the signal to frequency-wavenumber domain, where the signal and noises are well separated. The following can be removed by applying the apparent velocity filtering.

### 2.2.1. Definition:

The input seismic data was transformed from the conventional t-x domain to the f-k domain by 2-D Fourier transform. The 2-D Fourier transform separates events according to their dips in the f-k domain. A seismic section is a function of the variables time and distance  $s(t, x)$ , the passage from this plan  $(x, t)$  in the plan  $(f, k)$  is ensured by the double Fourier transform 2D-FT.

$$FT_{x,t}[s(t,x)] = FT_x\{FT_t[s(t,x)]\} = S(f,k) \quad (2.4)$$

Where:

$f$  : Temporal frequency.

$k$  : Spatial frequency (Wave number).

The bidimensional discrete Fourier transform BDFT is defined by the relation [7]:

Forward:

$$S(n_k, n_f) = \sum_{n_x=0}^{N_x-1} \sum_{n_t=0}^{N_t-1} s(n_x, n_t) e^{-j2\pi \left[ \frac{n_x n_k}{N_x} + \frac{n_t n_f}{N_t} \right]} \quad (2.5)$$

Where:

$n_t, n_f, n_x, n_k$ : The sample number in time, in frequency, in distance and wavenumber respectively.

$N_t, N_x$ : The number of samples in time and distance respectively.

This transform is well-known in seismic as  $(f, k)$  transform. It is used in seismic signal processing because its property of separation the signals in the  $(f, k)$  domain relating to the apparent velocity. This transform is particularly interesting for functions  $s(t, x)$  representing signals propagating at constant velocity  $v$  and observed on a regularly spaced grid of detectors,  $s(t, x)$  can then be written [7]:

$$s(t, x) = g(t - \frac{x}{v}) = g(t) * \delta(t - \frac{x}{v}) \quad (2.6)$$

If we elaborate on the operation of the 2D FT:

$$FT_t[g(t - \frac{x}{v})] = G(f) e^{-2j\pi f \frac{x}{v}} \quad (2.7)$$

Now performing the FT for the variable  $x$  gives:

$$FT_x[G(f) e^{-2j\pi f \frac{x}{v}}] = G(f) FT_x[e^{-2j\pi f \frac{x}{v}}] = G(f) \delta(k + \frac{f}{v}) \quad (2.8)$$

Modulus of the 2D Fourier Transform of  $s(t, x)$  gives the representation of the wave in the  $(f, k)$  plane as:

$$FT_{x,t}[g(t - \frac{x}{v})] = G(f) \delta(k + \frac{f}{v}) \quad (2.9)$$

In the plan of the two frequencies  $f$  and  $k$ ,  $\delta(k + \frac{f}{v})$  represents the straight line  $k + \frac{f}{v} = 0$  passing through the origin with slope  $(-v)$ . The wave velocity depends on frequency. Using the 2DFT, a positive apparent velocity ( $v = \frac{x}{t}$ ) in the  $(x, t)$  plan corresponds to a negative apparent velocity ( $v = -f/k$ ) in the plan  $(f, k)$ .

To obtain an apparent velocity with the same sign in both domains, the following transform can be done using the inverse  $x$  transform:

$$FT_{x,t}[s(t, x)] = FT_x \{ FT_t [s(t, x)] \} = S(f, k) \quad (2.10)$$

The double transform allows:

- Emphasizing the constant velocity events,
- Estimating velocities,
- Filtering out waves with various velocities, and
- Improving the signal-to-noise ratio.

The inverse bidimensional Fourier transform  $BFT^{-1}$  ensures the return in the initial domain [2]:

$$FT_{k,f}^{-1}[S(f, k)] = FT_k^{-1} \{ FT_f^{-1}[S(f, k)] \} = s(t, x) \quad (2.11)$$

The inverse is given by:

$$s(n_x, n_t) = \frac{1}{N_x N_t} \sum_{n_k=0}^{N_k-1} \sum_{n_f=0}^{N_f-1} S(n_k, n_f) e^{+j2\pi \left[ \frac{n_x n_k}{N_x} + \frac{n_t n_f}{N_t} \right]} \quad (2.12)$$

with:  $N_k, N_f$ : represent respectively the number of samples in wave-number and in frequency.

### 2.2.2. Signal and noise presentation in the plan (f, k):

The hyperboles of reflection are characterized by high velocity and located in the high frequencies, their projections in the field  $(f, k)$  are located near low wave number and are spread out over the axis of the frequencies. However, the noises (ground-roll) are characterized by their low apparent velocity and low frequencies. Thus their projections in the field  $(f, k)$  are located near high wave-number and low frequencies (Fig 2.1).

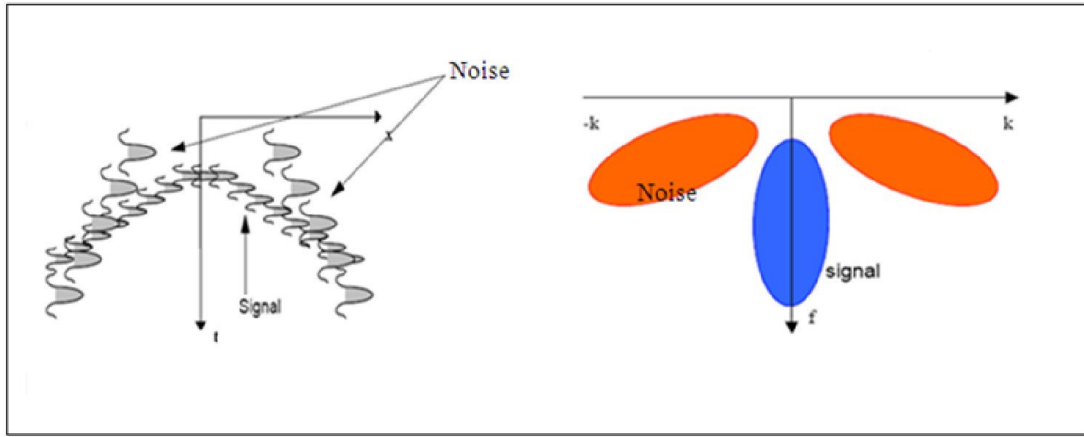


**Figure 2.1:** projection of a seismic section in the plan  $(f, k)$  [2]

### 2.2.3. $(f, k)$ filter procedure:

The position of the undesirable events in the domain  $(f, k)$  will be related to their characteristics, and will allow determining the type of the filter to be used to improve the signal to noise ratio. The choice of filtering will thus depend on the position of the signal and the noise on the spectrum  $(f, k)$

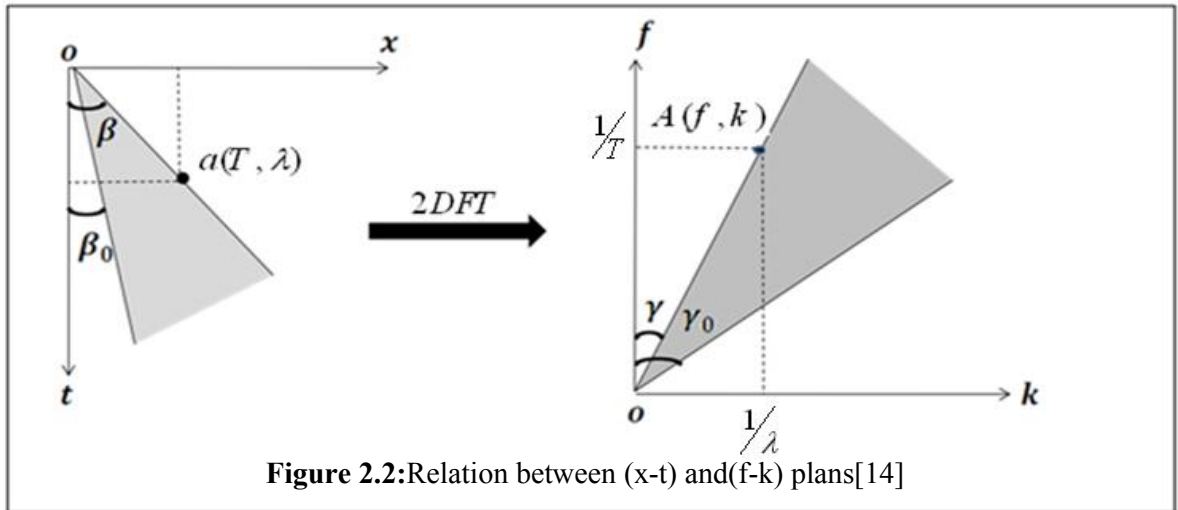


**Figure 2.2:** Relation between  $(x-t)$  and  $(f-k)$  plans [14]

Considerin seismic section, a seismic arrival  $a$  characterized by a period  $T$  and wavelength  $\lambda$  corresponds to a noise of apparent velocity  $v_a = \tan \beta$ . The representation of this point in  $(f, k)$  domain is a point  $A(f = 1/T, k = 1/\lambda)$ , so its tangent is  $v_a = f/k$ .

$\tan \gamma = \frac{1}{v_a} \Rightarrow \tan \gamma = \frac{1}{\tan \beta} \Rightarrow \gamma = \frac{\pi}{2} - \beta$ . Therefore, the filtering of the events having a tangent greater than  $\tan \gamma$  in  $(f, k)$  domain is the same as filtering the arrivals of apparent velocity  $v_a$  less than  $\tan \beta$ . In the same manner if we filter the events lying inside the angle  $(\gamma_0 - \gamma)$  in  $(f, k)$  domain, we remove the arrivals having the apparent velocities lying between  $(\beta - \beta_0)$ . This type of filtering is known as apparent velocity filtering.

There exist other types of frequency wavenumber  $(f, k)$  filtering :

- Frequency filtering
- Wavenumber filtering
- Polygon filter
- Strip filter

## 2.3 AGORA modeling

In this part we present a data driven approach that performs an adaptive filtering of aliased and dispersive Surface Waves at their true spatial coordinates (AGORA). This approach uses the ground roll characteristics contained in each shot (group and phase velocities) to perform an Elastic Modeling of the “signal” and “noise (Surface Waves)” in the FX domain for several frequency bands.

### 2.3.1 Technical background:

If we analyze several shots from the same survey, we observe that the characteristics of the ground roll (GR) changes from one shot location to another with respect to their dispersion properties (see **Figure 2.3-a, b**). Maps of the main mode of the GR for non-aliased frequencies can easily be made to highlight significant spatial variation of the GR velocity reaching up to a factor of 4 at short distances (see **Figure 2.3- a**). Observations and measurements on records indicate a real change in the GR characteristics (frequency content, phase velocity, amplitude and degree of aliasing) (see **Figure 2.3-a, e**). This is the reason why the GR characteristics should be taken into account and the group and phase velocities extracted from each record to feed the anti-noise filtering. Our anti-noise filtering is based on an Elastic Modeling in the FX domain using the true distance between the source and the receiver (irregular spatial sampling). The principle is that the input data is a mixture of signal plus coherent and incoherent noise (see Perkins and Zwaan, 2000). The signal (S) is modeled as hyperbolic events whose trajectories are described by stacking velocity (V-rms) (see **formula 2.13**). The coherent noise (GR) is modeled



as a series of dispersive linear events, each distinguished by group and phase velocities (**see formula 3.16**)[15]

$$S_{(j,k)} = e^{i \cdot f \sqrt{t_j^2 + \frac{X_k^2}{V_{rms}^2}}} \quad (2.13)$$

$$GR_{(j,k)} = e^{i \left( \frac{f_0}{V_{pj}} + \frac{f-f_0}{V_{gj}} \right) X_k} \quad (2.14)$$

$J^{th}$  eventis: the zero offset travel time

$X_k$ : is the true shot to receiver distance.

$f_0$  : is the central frequency of the wave.

$V_{pj}$  and  $V_{gj}$  are the phase and group velocities extracted from the input data.

These events form the components of the matrix **A** with column and row indices  $j$  and  $k$ .

In the frequency domain, the input data is represented by a matrix **D** which can be described by a matrix **A** that contains the dispersive linear and hyperbolic events multiplied by a vector **W** containing an unknown wavelet corresponding to the signal and GR plus a percentage of random noise **N** (**see formula 3.15**).

$$D = A \cdot W + N \quad (2.15)$$

$$A = \begin{bmatrix} e^{i \cdot f \sqrt{\frac{t_0^2 + X_1^2}{V_{rms}^2}}} & e^{i \left( \frac{f_0}{V_p} + \frac{f-f_0}{V_g} \right) X_1} \\ \dots & \dots \\ e^{i \cdot f \sqrt{\frac{t_0^2 + X_n^2}{V_{rms}^2}}} & e^{i \left( \frac{f_0}{V_p} + \frac{f-f_0}{V_g} \right) X_n} \end{bmatrix} \quad (2.16)$$

$$D = \begin{bmatrix} D(f, x_1) \\ \dots \\ D(f, x_n) \end{bmatrix} \quad (2.17)$$

$$W = \begin{bmatrix} W(f, x_1) \\ \cdots \\ W(f, x_n) \end{bmatrix} \quad (2.18)$$

Rewriting formula (3.15) in appropriate terms, a least squares iterative inversion approach is used to extract the GR from the input data. Notice that this scheme is efficient if the current frequency is reasonably close to the defined central frequency. However, in most cases the GR may have a bandwidth of more than 30 Hz! This dilemma, however, is resolved by splitting the data into several frequency bands that allows the use of several different central frequencies in order to optimize the modeling of the coherent noise.

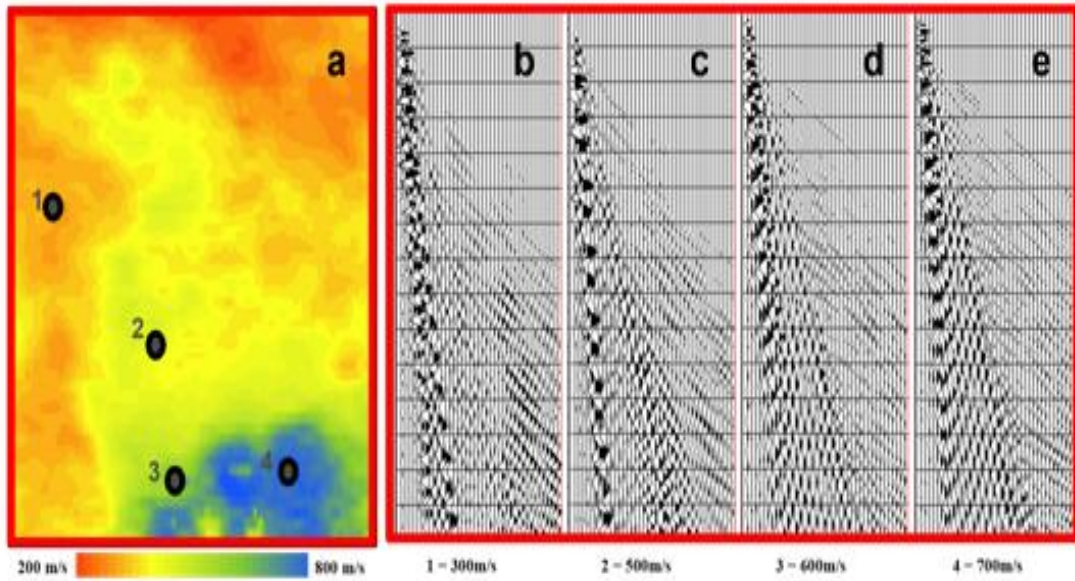


**Figure 2.3:** GR velocity map with record locations, b-e) the corresponding shot records.

### Data examples:

This adaptive anti-noise attenuation method is now applied to two data sets to demonstrate its effectiveness. The first example contains two receiver cables, a central and a broadside cable, extracted from a 3D shot record (**Figure 2.4**). The top row of (**Figure 2.4**) shows the central cable and the bottom row the broadside cable. From left to right, we have successively the raw receiver cable, the receiver cable after the adaptive filtering and the difference of both. On both raw receivers high-amplitude dispersive GR energy is clearly visible with weaker primary reflection events crossing the GR cone (**Figure 2.4-a, c**). After the adaptive filtering the GR energy has been removed, but the weaker reflection events remain the same (**Figure 2.4-b, e**). Black arrows highlight the fact that no signal leakage appears on the difference panels (**Figure 2.4-a, c**) but that only linear or dispersive GR have been suppressed. The second example shows the efficiency of

the filtering process on 2D data. From top to bottom are displayed the raw stack, the stack after the adaptive filtering (on the raw input shots) and the stack of the noise that has been removed (difference stack). On the raw stack high amplitude dipping events cross and partially cover the shallow section and the main primary events (**Figure 2.5**). After the GR filtering on the raw shots the high amplitude low frequency GR has been completely removed allowing us to see the continuity of the shallower weak primaries at around 1 s TWT (**Figure 2.6**). There is no signal leakage on the stack of the noise although some pseudo-coherent events appear due to a constructive stack of the GR.

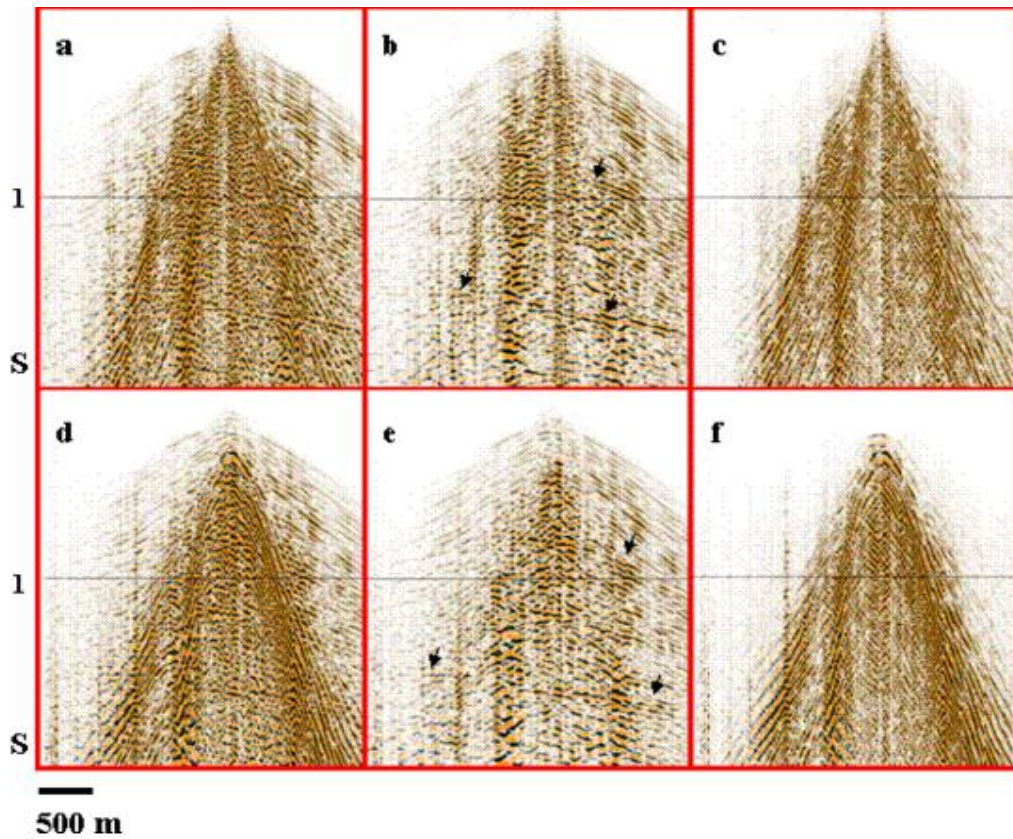


**Figure 2.4:** a) raw input central cable, b) filtered central cable, c) difference between a) and b) d) raw input broadside cable, e) filtered broadside cable, f) difference between d) and e)



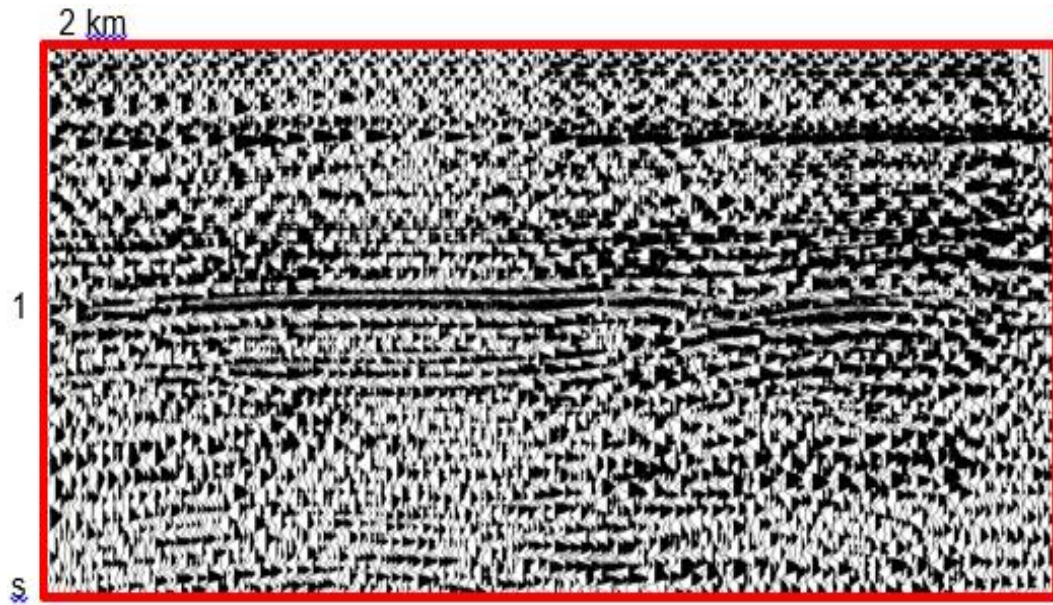


Figure 2.5: Stack of the input data

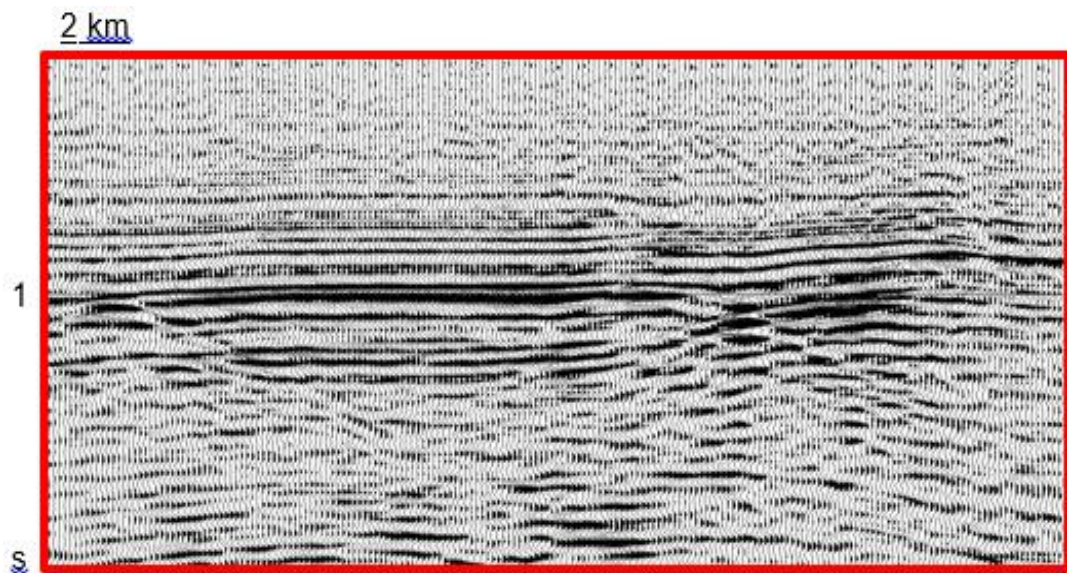
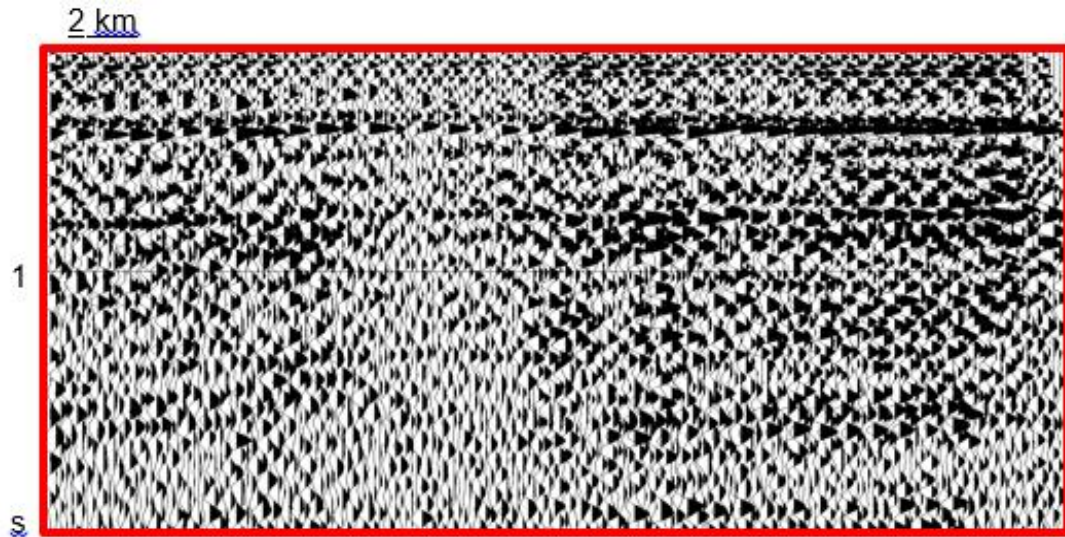


Figure 2.6: Stack after an adaptive filtering of the GR on raw shots



**Figure 2.7:** Stack of the noise removed during the adaptive filtering

## 2.4. Summary:

In this chapter, we explained the sampling process of the seismic function on the ground, as well as the consequence of this sampling, which is the spatial filtering of the seismic function. In addition, we have described the theory and principle of filters, the most used in seismic oil. Currently, we are going to apply these two filters on real seismic signals and the results will be exposed in the next chapter.

## Introduction:

Throughout this chapter, we present the different results obtained after the applications of the filters ( $f$ ,  $k$ ) and AGORA on seismic data (Real data).

The aim of this part is to study the effectiveness, the advantages and the limits of application of these two filters. For this reason, we carried several tests on the real data varying the velocity, attenuation coefficient, and the frequency. The different handlings were made by the workstation GEOVISION, during our training in the department of processing at ‘‘E.N.A.GEO’’ (Enterprise National De Géophysique).

### 3.1. Geological framework of the region:

The Negrine region located in the Constantine basin with a surface area of 8184.44 km<sup>2</sup>, called Block 126, has 12 exploration wells and 5 delineation wells (Figure 3.1).

The South East Constantine Basin, corresponds to a subsidizing sedimentary basin whose history begins at the end of the Triassic and ends at the Tertiary. It includes a strongly folded atlas area and a stable domain (chottmelrhir). The SE Constantine basin is characterized by:

- An intense Triassic diapirism which is set up along the major NE-SW accidents, as well as at the intersection of these with NW-SE transverse accidents.
- An alignment of the trends in the NE-SW direction with narrow anticlinal folds separated by large plains Miocene-Pliocene and Quaternary. Intense fracturing is represented by NE-SW longitudinal and NW-SE transverse faults (Figure 3.2).

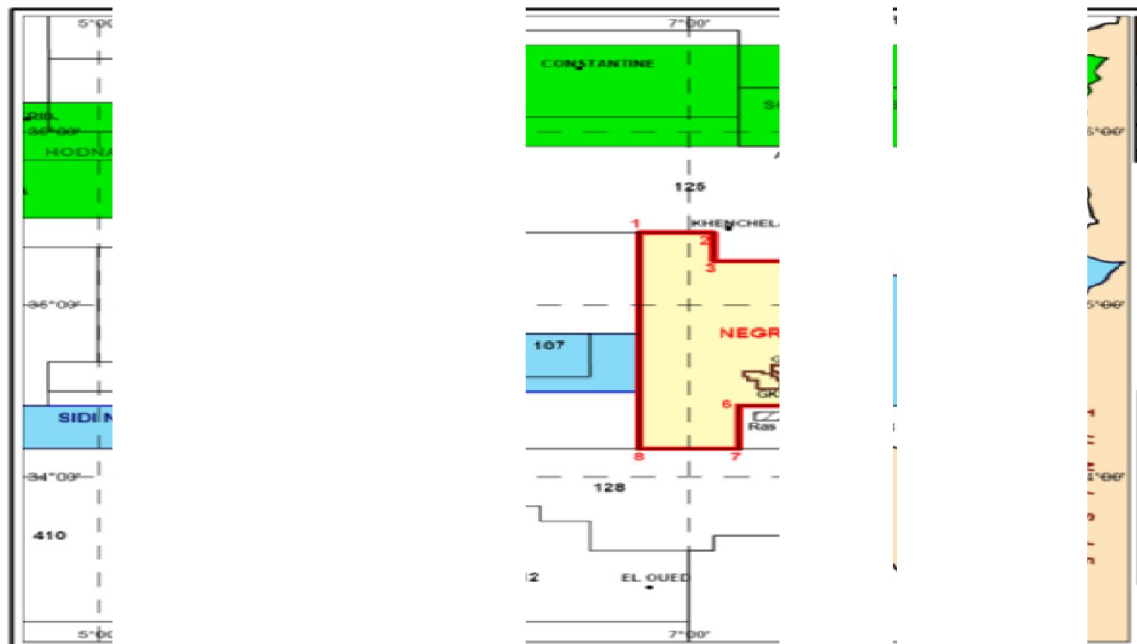


Figure 3.1: NEGRINE region Location.



### 3.2. Description of the study profile:

Our profile 16NG04 is located in the north of the NEGRINE 2D project (Figure3.3), this profile contains 2615 firing points with a length of 65.375 km, 105 fire points are skipped because of mountains, forests and the effect of altimetry (Figure3.4).

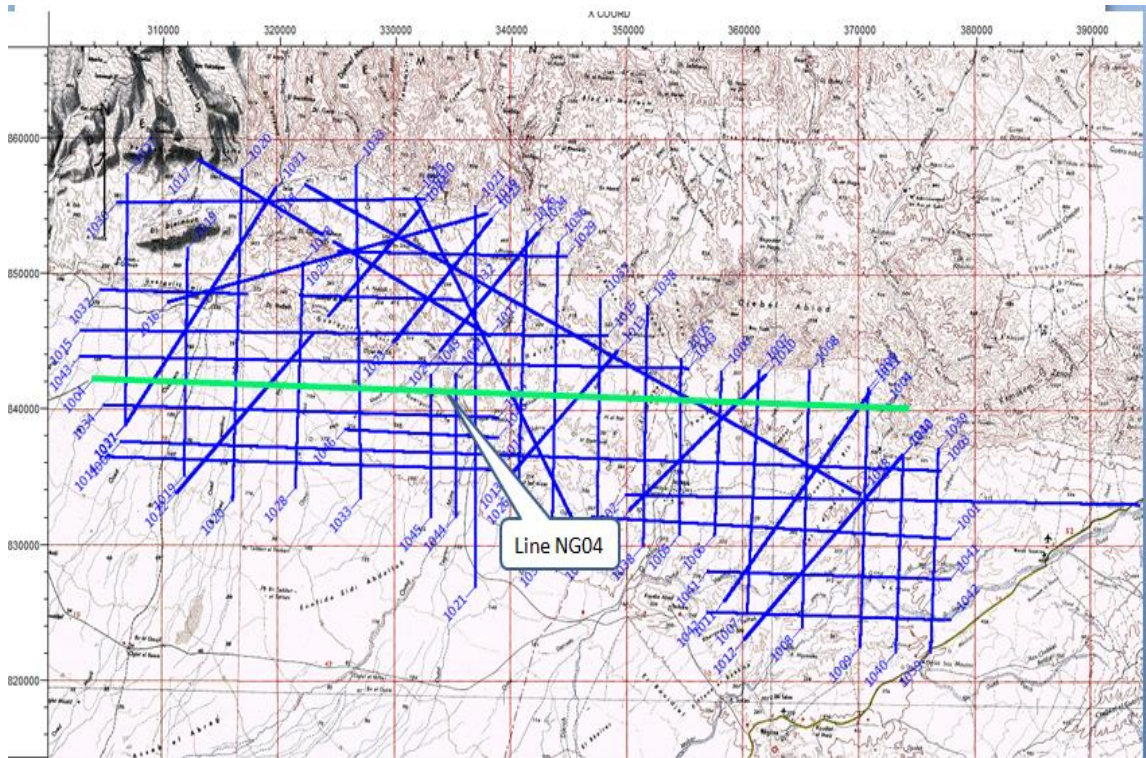


Figure 3.3: 16GN04 profile location map of block 126.

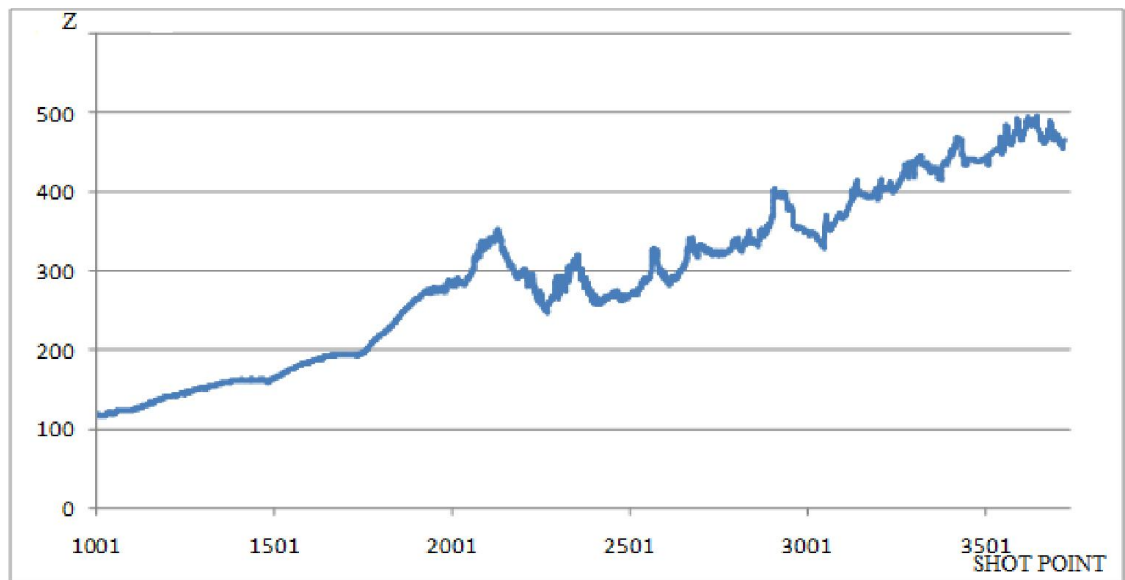


Figure 3.4: Elevation graph of the 16GN04 profile surface.

### 3.3. Acquisition parameters:

The acquisition parameters used by the seismic campaign include the following parameters:

#### 3.3.1. Recording parameters:

- ✚ -Recording system: sercel 428XL
- ✚ Recording format: SEG-D
- ✚ Sampling interval: 2ms
- ✚ Recording length: 5s
- ✚ Anti-aliasing filter: 0.8 Nyquist, linear phase
- ✚ noise edit: off

#### 3.3.2. Source parameters:

- ✚ -Source Type: vibros, I / O AHV IV
- ✚ -Number of vibros: 4
- ✚ -Number of Sweeps: 3
- ✚ -Sweep length: 12 seconds
- ✚ -Sweep frequency band: 6 - 72 Hz
- ✚ energy level: 80%
- ✚ -The total mass: 62000
- ✚ -Rotation phase between sweeps: No
- ✚ -Model Sweep: Move up
- ✚ -Move up: 7 meters
- ✚ -Distance between Vibros: 17 meters
- ✚ -the storing type of the vibros: Linear
- ✚ -Length of storage: 65 meters

#### 3.3.3. receiving parameters:

The arrangement of the receiving layer is shown in (Figure 3.5).

- ✚ -Geophone Type: SN7C-10
- ✚ -Geophones by Trace: 2 strings (6 geophones in 1 string)
- ✚ -Type of storing geophones: Linear
- ✚ geophones interval: 2.08 meters
- ✚ -tidy Length: 22.91 meters



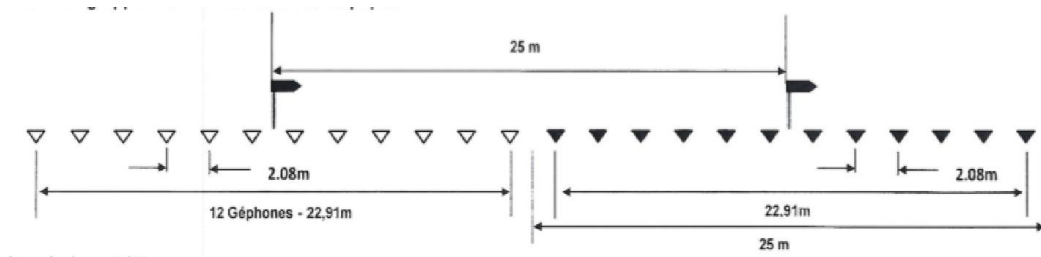


Figure 3.5:geophones Arrangement in the field.

### 3.4.random noise Attenuation:

The shot 1004 of the profile 16NG04 and the seismic section of this profile were chosen for analysis. The analysis on shot and raw stack shows that the random noises are very aggressive and completely masking the useful signal and even the organized noise which requires the attenuation of the random noises in order to pass to the organized noise filtering (Figure 3.7 and 3.9). The attenuation of random noise is achieved by two stages of treatment: the editing of noisy traces and Despiking.

#### 3.4.1.Trace editing:

On the time window between 4s and 5s, we calculated the RMS amplitude for each trace along the profile (Figure 3.6). Traces outside the maximum population are considered noises. They are edited after having their selections.

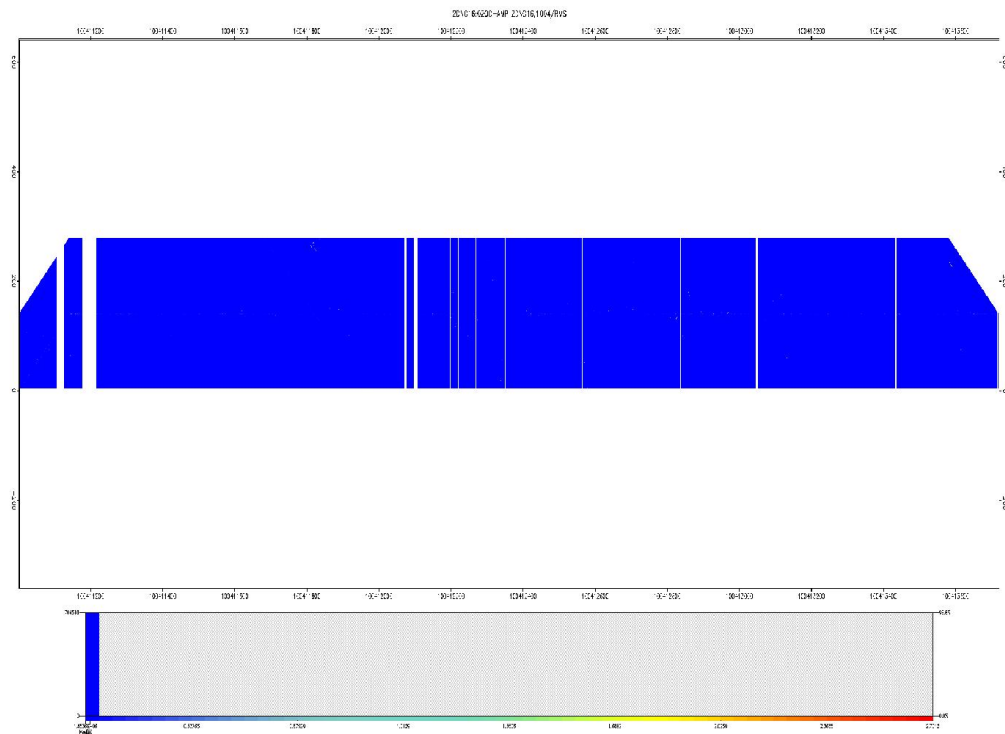


Figure 3.6:RMS amplitude of the 16NG04 profile.

### 3.4.1.1.resultsAnalysis and comparison:

#### • Onshot and stack:

Stack analysis shows that noisy traces are eliminated, reflections and linear noises appeared (see Figure 3.8).The analysis of the shot 1004 edited shows a better result of the noisy traces this confirms the importance of random noise attenuation in the treatment. But there are traces that are not edited because they are outside the edition window (see Figure3.10).

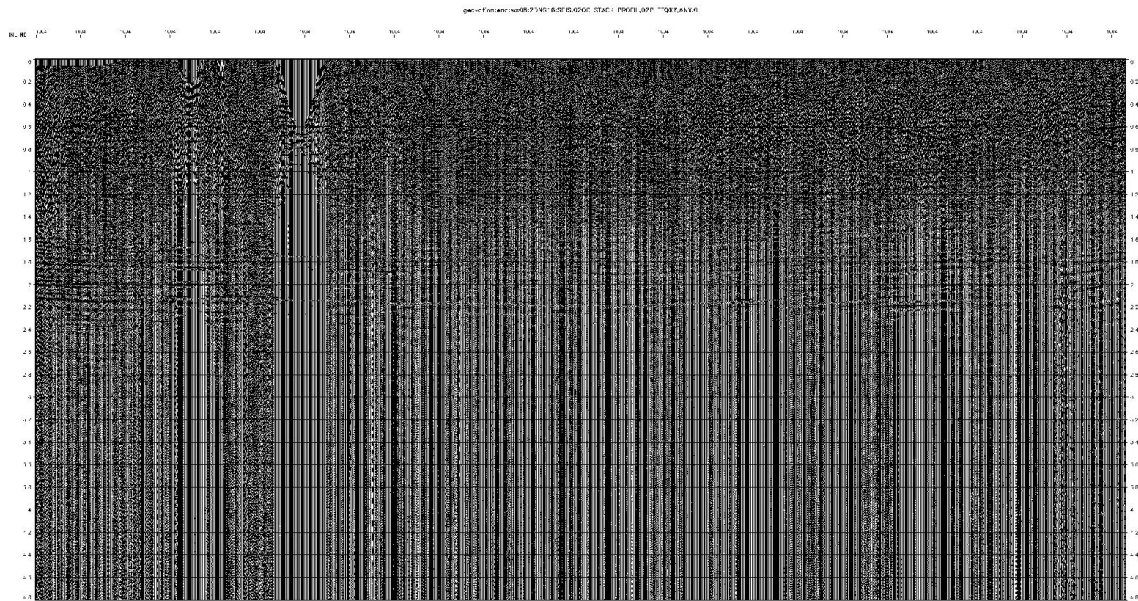


Figure 3.7:Raw stack of the 16NG04 profile.

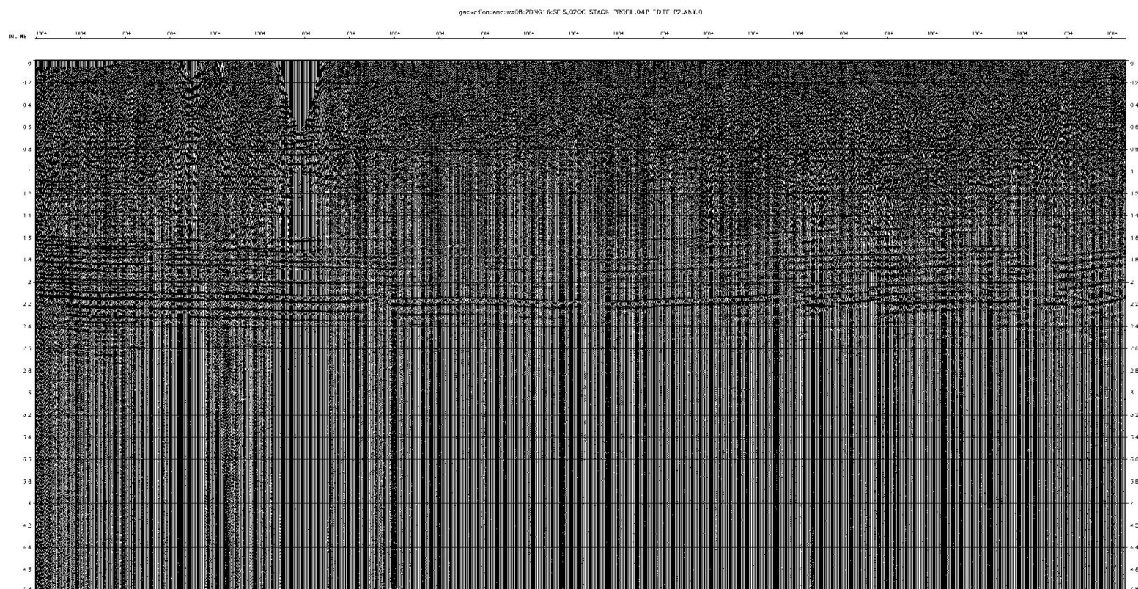


Figure 3.8:Stack of the 16NG04 profile after editing.



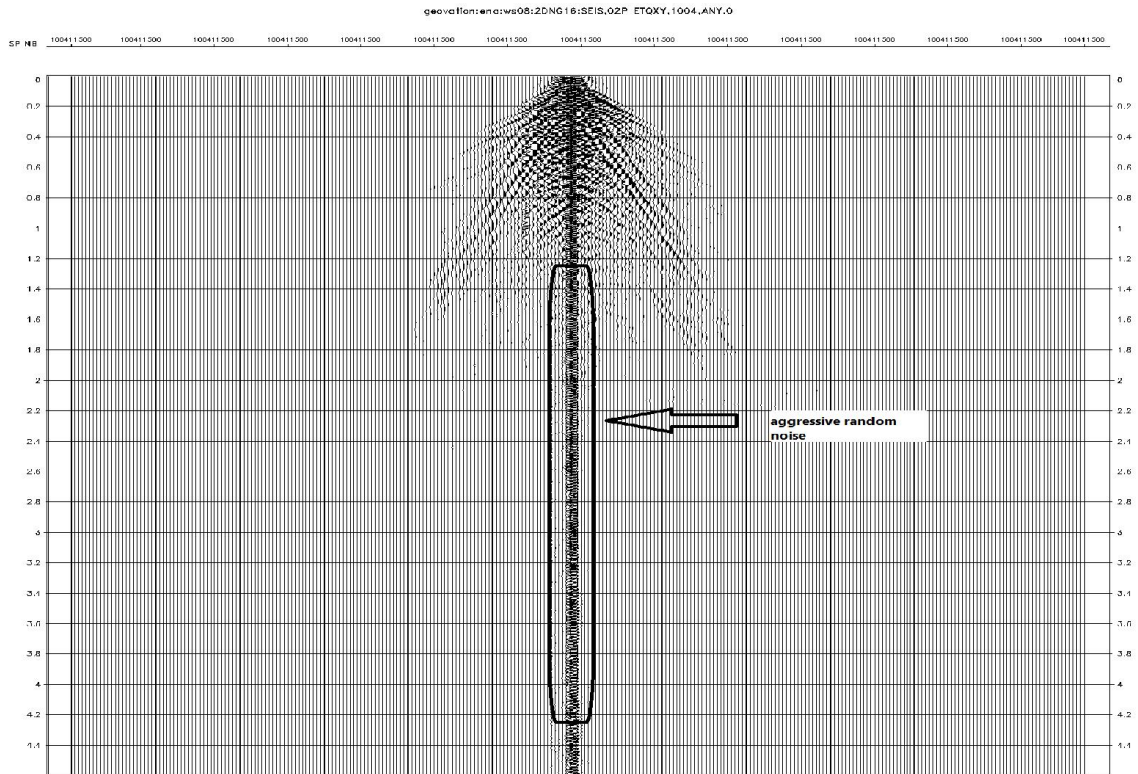


Figure 3.9: Raw shot 1004.

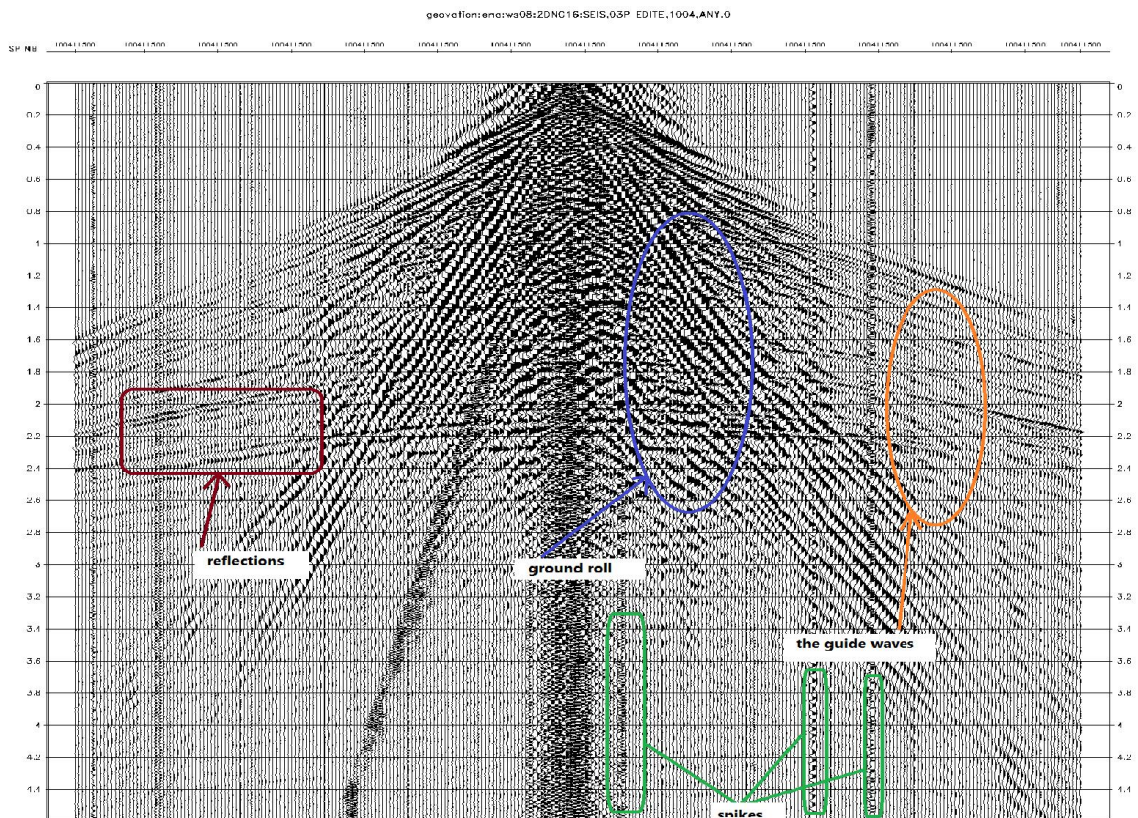


Figure 3.10: The shot1004 after editing.

### • On spectrum:

Analysis of the amplitude spectra of the shot 1004 and the stack before and after editing show:

- ✚ low noise attenuation for low frequency traces
- ✚ high attenuation for the high frequencies (**Figure 3.11 and 3.12**).

and this shows the efficiency of the trace editing attenuation operation on the aggressive noises that have high frequencies, and it preserves the traces with low frequencies.

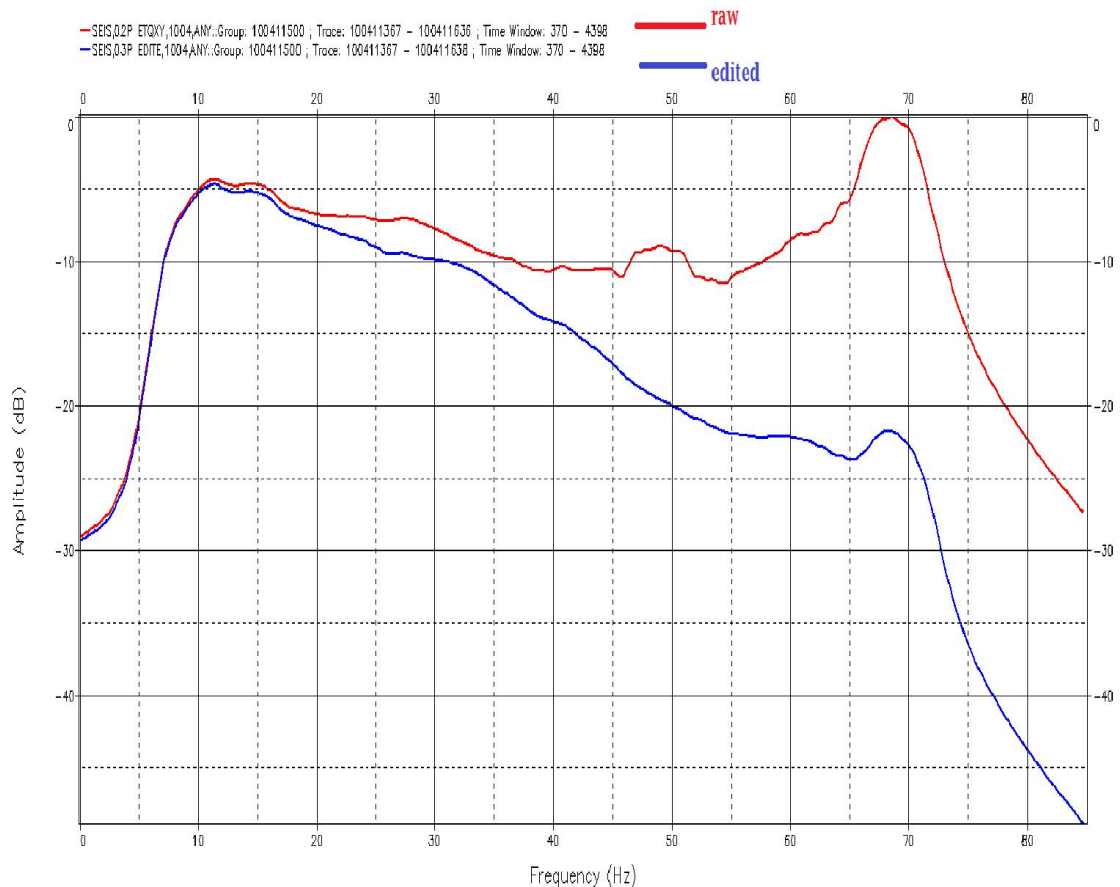


**Figure 3.11:**Amplitude spectrum before editing and after.

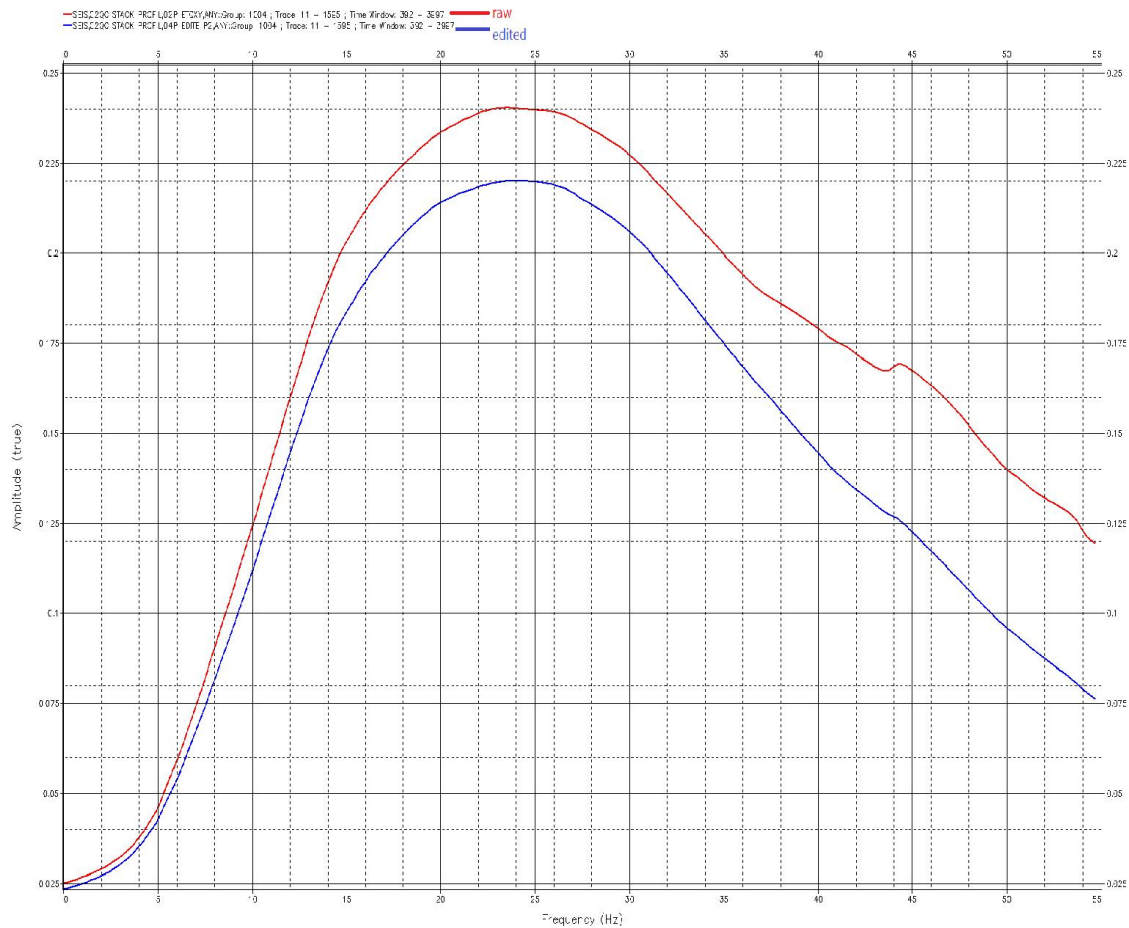


**Figure 3.12:** Amplitude spectrum for the 16NG04 profile stack before and after editing.

### 3.4.2. Despiking:

The Spike is a random noise which can be identified on shot, characterized by a high amplitude. The location and elimination of the spikes is very important in signal processing.

Spikes are usually difficult to identify by existing algorithms because they have features which often are quite similar to those of real earthquake signals. The majority of conventional despiking algorithms require empirical tuning of associated parameters. The required parameter tuning often degrades the efficiency of automated algorithms, which in the end do not save much time and effort when compared with manual approaches. Hence, most despiking is done by direct manual editing, which can be a rather monotonous task, especially when one deals with a large dataset which is our case.



### 3.4.2.1 results Analysis and comparison:

- **Onshot and stack :**

After the analysis of the edited shot 1004, we have located some spikes (Figure 3.13). The elimination of those spikes cause to appear other signals that have been masked by these spikes (see Figure 3.14). The results obtained on stack show the appearance of reflectors and linear noise in the window between 2.5s and 4.5s, which shows the importance of spikes elimination before attenuation of linear noise (see Figure 3.15 and 3.16).

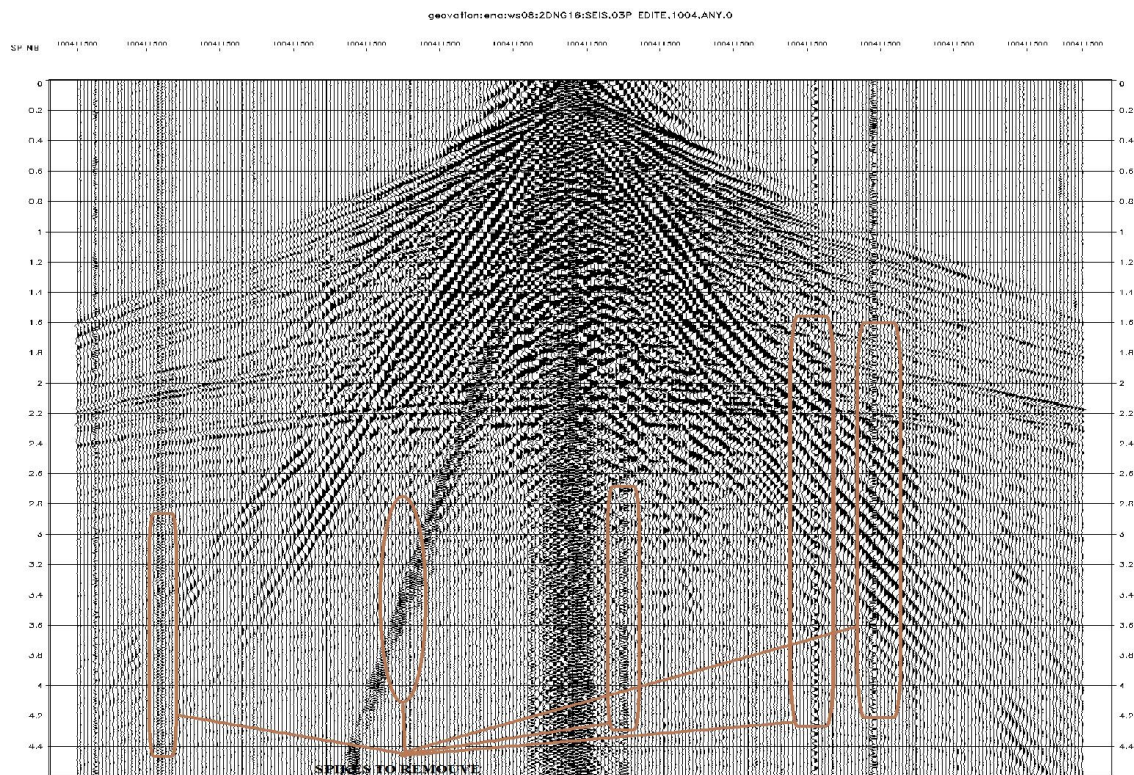


**Figure 4.13:** Location of spikes on shot 1004 after Edition



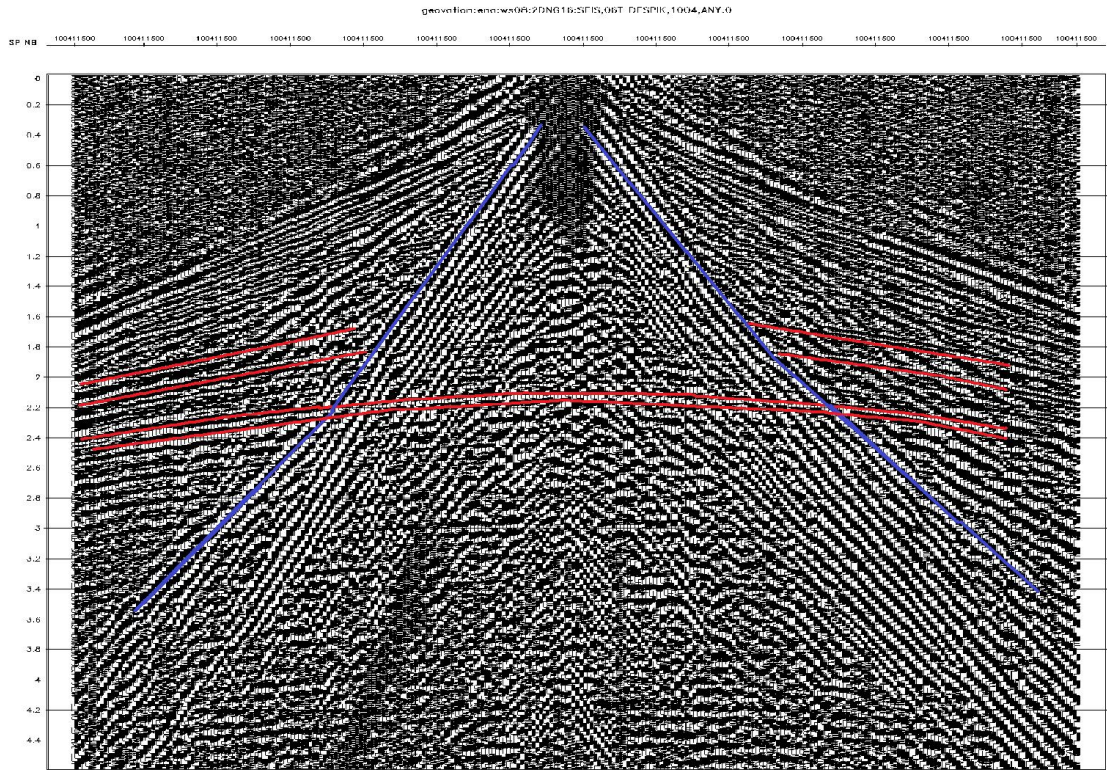


Figure 3.14: Shot 1004 after Despiking.

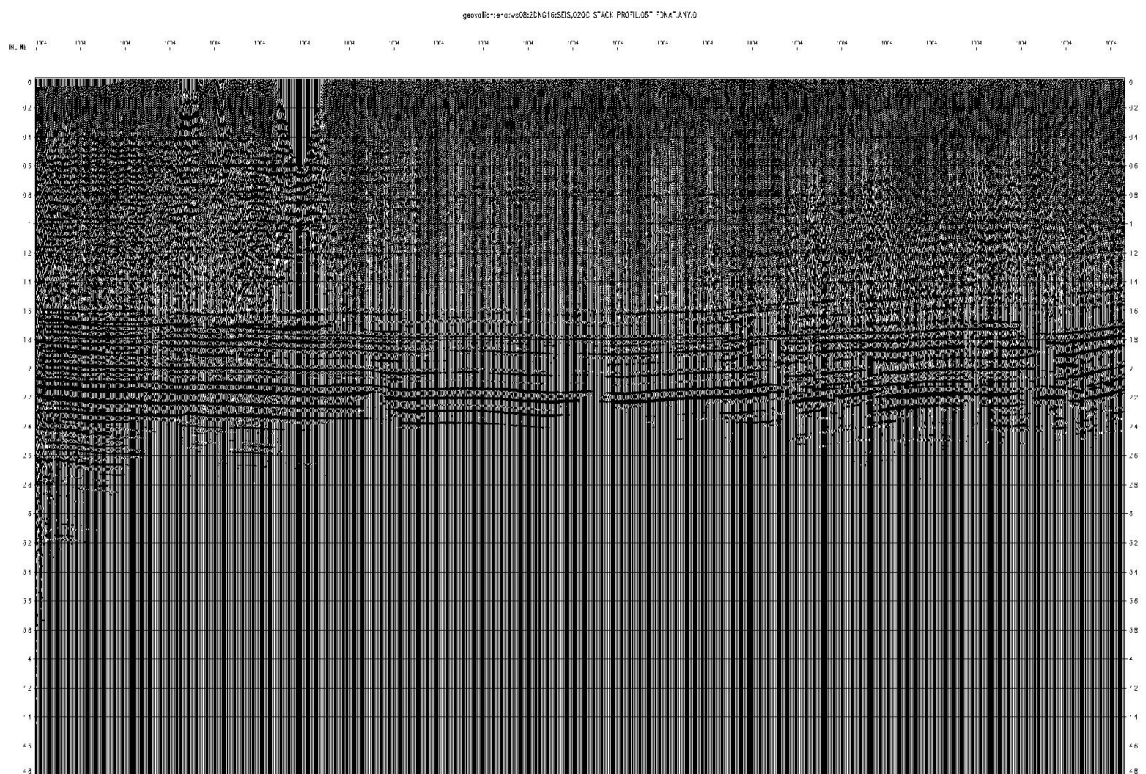


Figure 3.15: Stack of the 16NG04 profile before Despiking



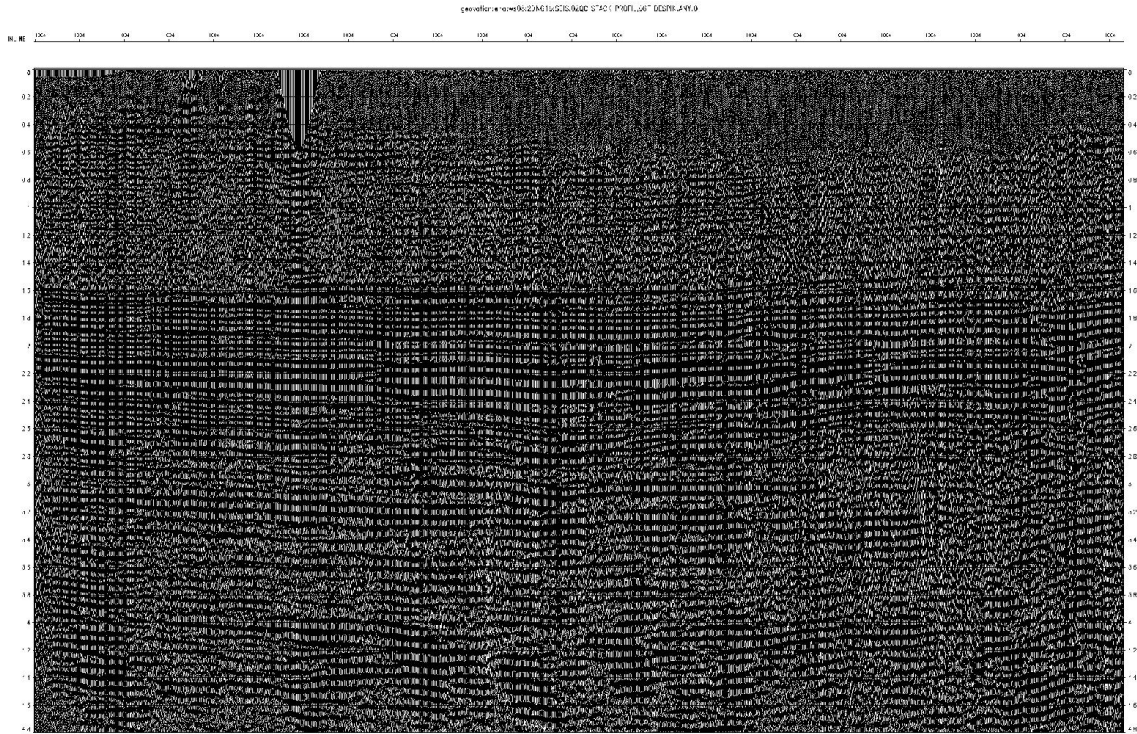
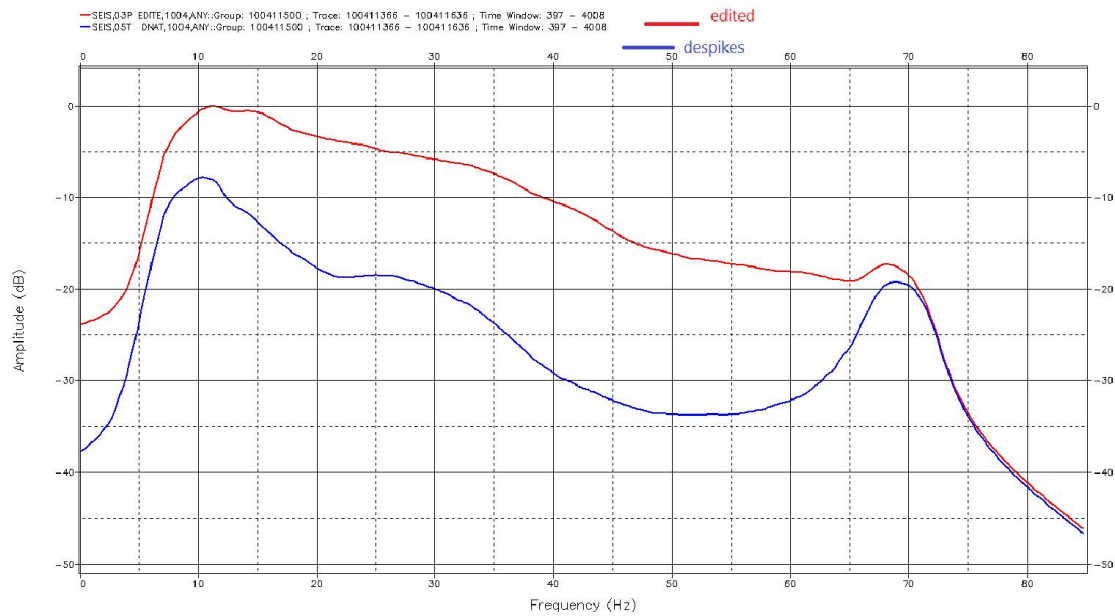


Figure 3.16: Stack of the 16NG04 profile after Despiking.

- **On Spectrum :**

The amplitude spectrum curve for shot 1004 after Despiking shows a large attenuation of the trace amplitudes in the [10-70] Hz frequency band and a weak attenuation outside this band (*Figure 3.17*). The spikes are characterized by a very high energy masking the other events, after the elimination of the latter the energy of the reflections and organized noises increase which explains the appearance of the reflections and organized noises.





**Figure 3.17:** Amplitude spectrum for shot 1004 before and after Despiking

### 3.5. Ground rollAttenuations:

Our oil objectives are in the window (2s and 4s), so we limited our analysis on this window, in order to have an interpretable seismic section it is necessary to attenuate ground rolls (seeFigure 3.18). The Figure 4.19 shows the presence of linear noise such as the direct wave, the refracted wave and the ground rolls that affect the seismic recordings, as well as the reflected waves (hyperbolic wave) embedded in the ground rolls. On this record, the apparent velocity of the ground roll varies between  $V = 500 \text{ m / s}$  and  $V = 2200 \text{ m / s}$ , these apparent velocity values are the slopes of the alignments that correspond to the ground-roll.

The attenuation of the ground roll will be affected by (f, k) filtering and AGORA modeling.

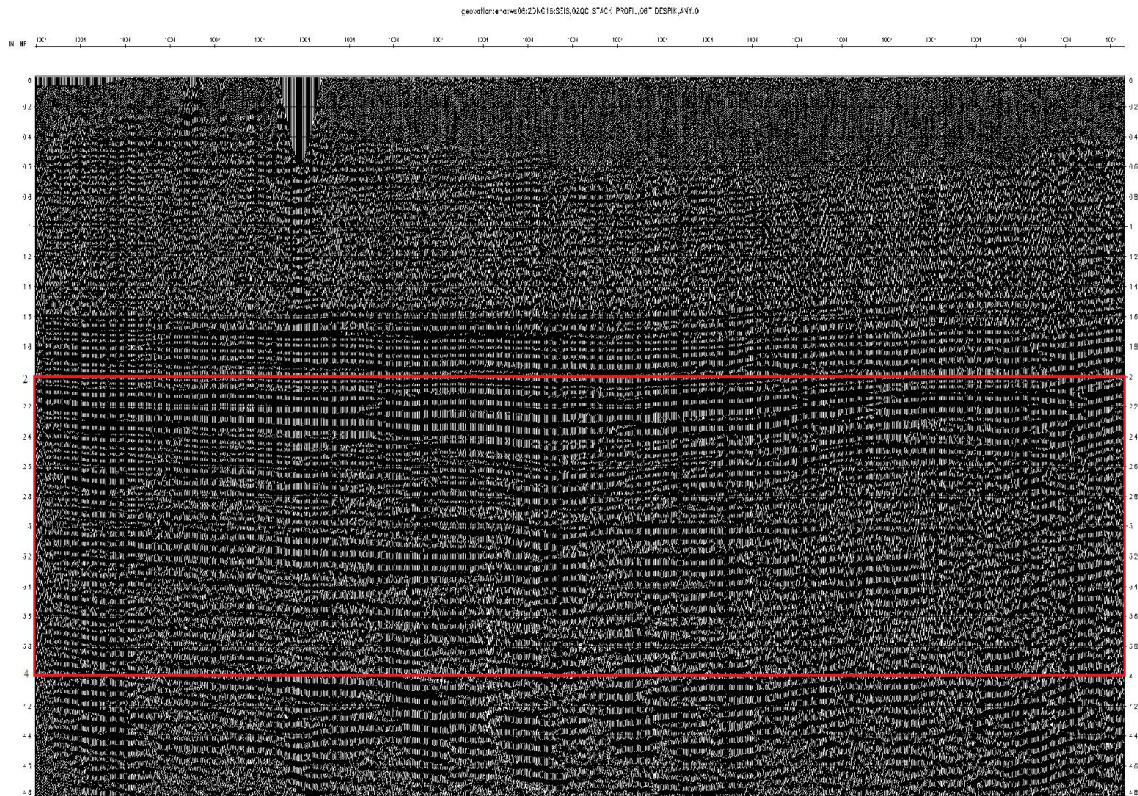


Figure 3.18: the stack of 16NG04 profile shows the target area.

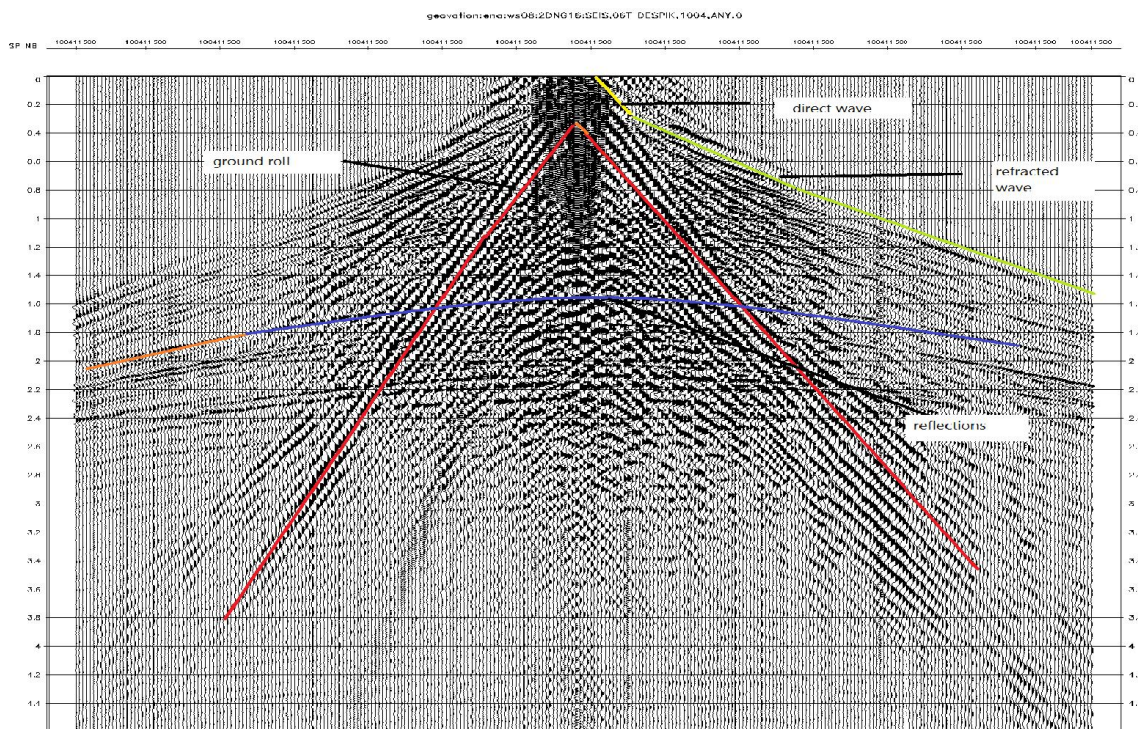


Figure 3.19: Representation of the different events on shot 1004 after the attenuation of the random noises.

**3.5.1. Attenuation by (f, k) filter:**

In this part, the filtering method applied is fan filter in (f, k) domain, after several tests on the shot 1004 filtered random noise. we chose two velocities  $V1 = 50 \text{ m / s}$  and  $V2 = 2000 \text{ m / s}$  for the limitation of the attenuation window of the ground rolls with attenuation coefficient  $E = 36$ . The choice of these parameters is done after analyzing the results on shot, stack and amplitude spectrum. These parameters are chosen based on the conservation of the useful signal and the attenuation of the ground roll (See Table 1).

**Table 1 : Tested parameters.**

<b>V1</b>	<b>V2</b>	<b>E</b>
<b>50</b>	<b>500</b>	<b>6</b>
<b>50</b>	<b>1000</b>	<b>6</b>
<b>50</b>	<b>1500</b>	<b>6</b>
<b>50</b>	<b>2000</b>	<b>6</b>
<b>50</b>	<b>2500</b>	<b>6</b>
<b>50</b>	<b>3000</b>	<b>6</b>
<b>50</b>	<b>3500</b>	<b>6</b>
<b>50</b>	<b>2000</b>	<b>12</b>
<b>50</b>	<b>2000</b>	<b>18</b>
<b>50</b>	<b>2000</b>	<b>24</b>
<b>50</b>	<b>2000</b>	<b>36</b>
<b>50</b>	<b>2000</b>	<b>48</b>
<b>50</b>	<b>2000</b>	<b>64</b>
<b>50</b>	<b>2000</b>	<b>72</b>
<b>50</b>	<b>2000</b>	<b>80</b>



### 3.5.1.1. Discussion and results:

#### • On shot and stack:

The comparison of shot 1004 before and after the (F, K) filter application shows that the ground rolls are attenuated and the reflections are well identified on the upper part of our data (see Figure 3.20 and 3.21). In parallel, the stack analysis confirms that the reflectors can be identified in the parts where the ground rolls are better attenuated, therefore there is a good continuity of the reflectors (see Figure 3.22 and 3.23).

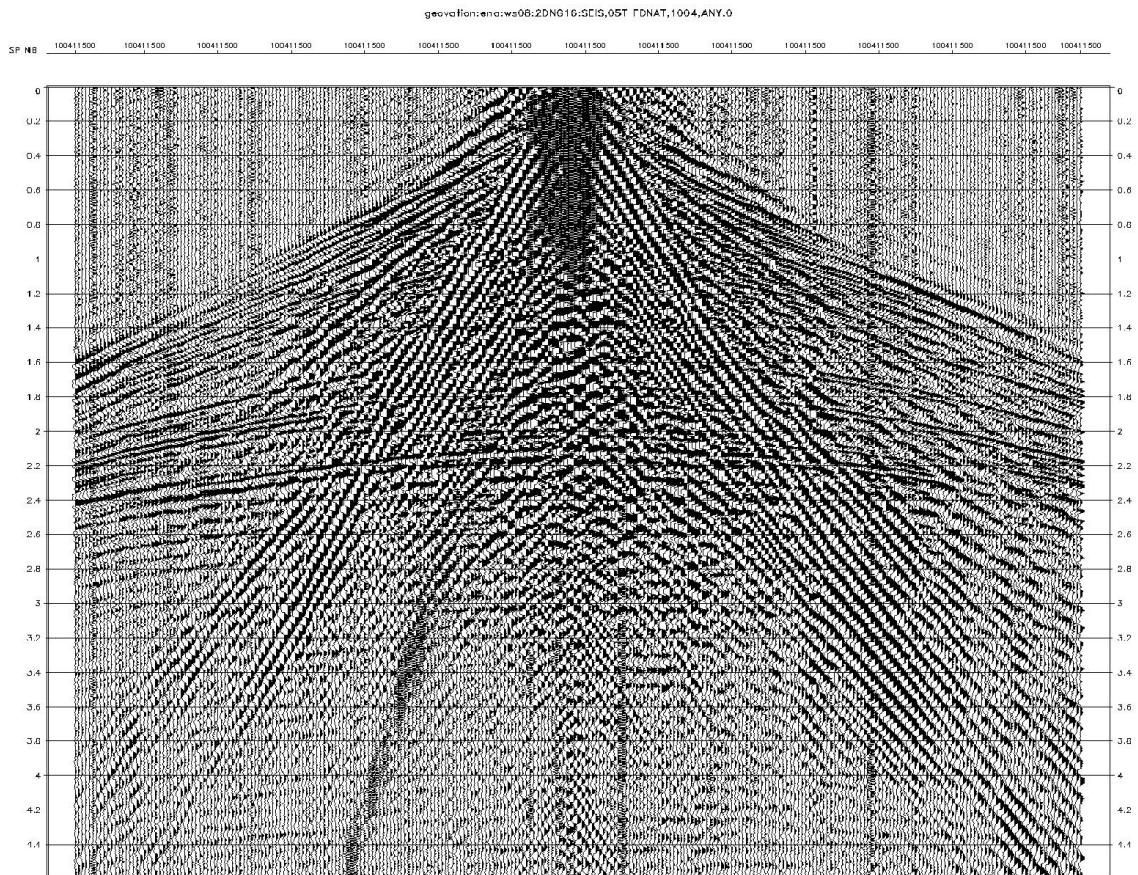
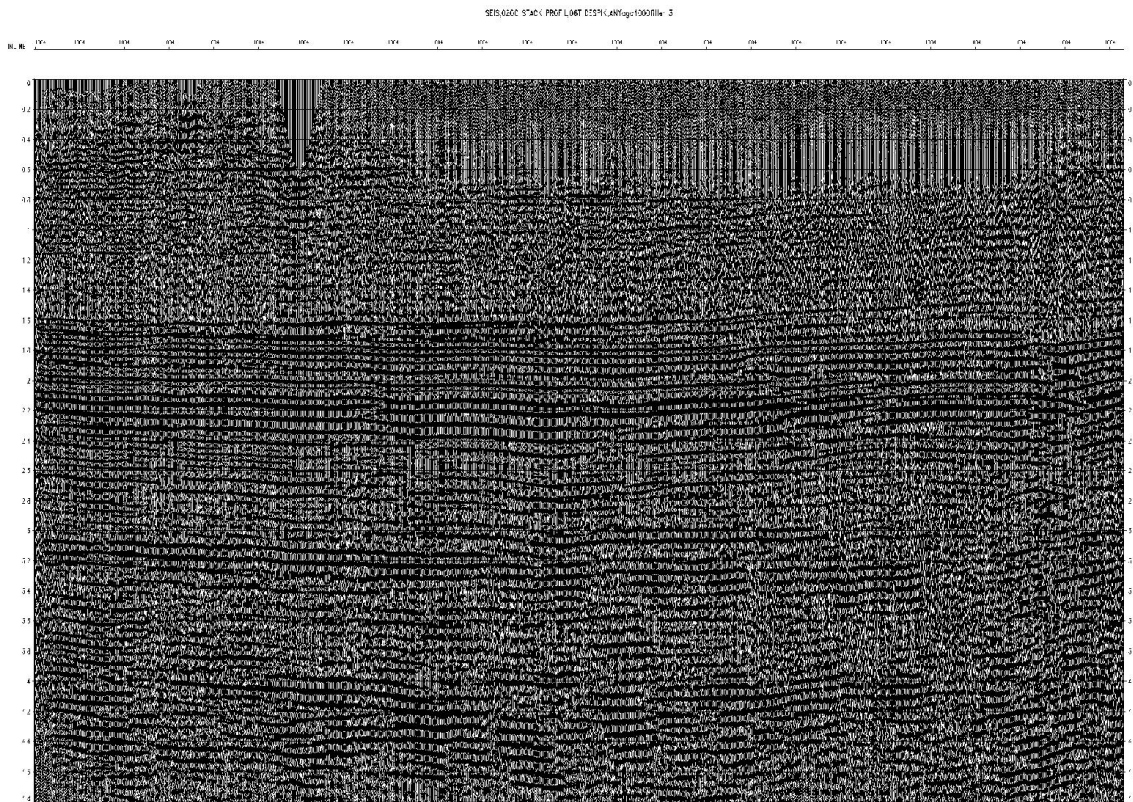
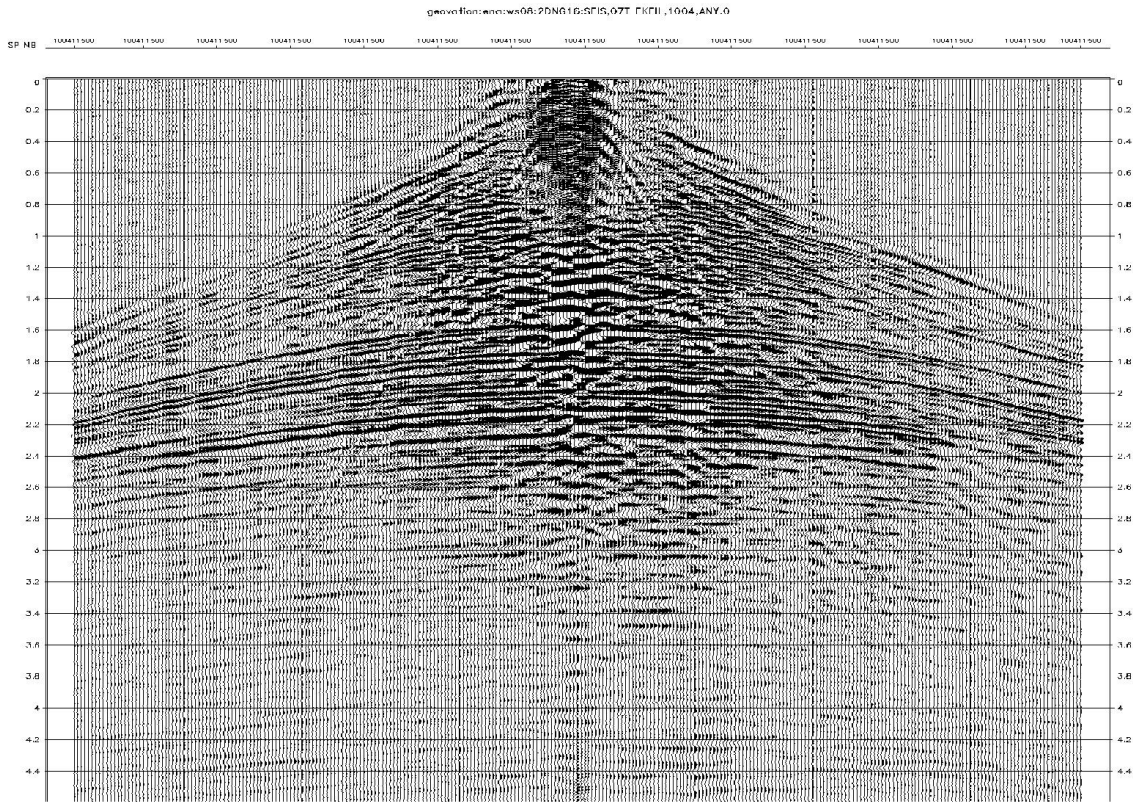


Figure 3.20: Shot 1004 before (f,k) filtering.









- **On Spectrum :**

On the representation of shot 1004 in the  $(f, k)$  domain, the signals have a velocity greater than  $2000 \text{ m/s}$  are close to the frequency axis considered as reflections. After the application of the  $(f, k)$  filter on this shot, the signals which have an apparent velocity lower than  $2000 \text{ m/s}$  are attenuated (see Figure 3.25 and 3.26).

After the analysis and comparison of the results obtained in the spectral domain, one concludes that the filtering in the field ( $f$ ;  $k$ ) is a method which is not effective enough on the ground roll attenuation which requires to seek for another methods more effective.

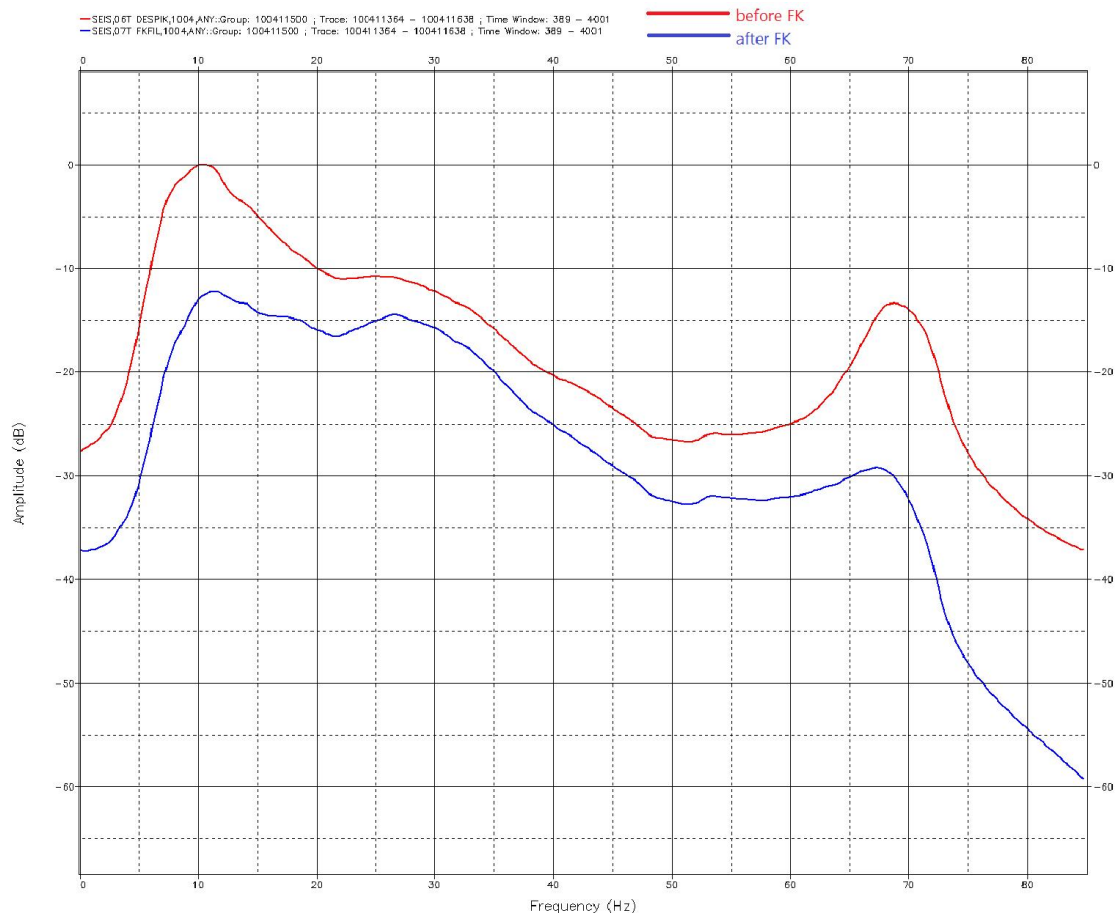


**Figure 3.24:**Amplitude spectrum before and after ( $f$ ,  $k$ ) filtering.

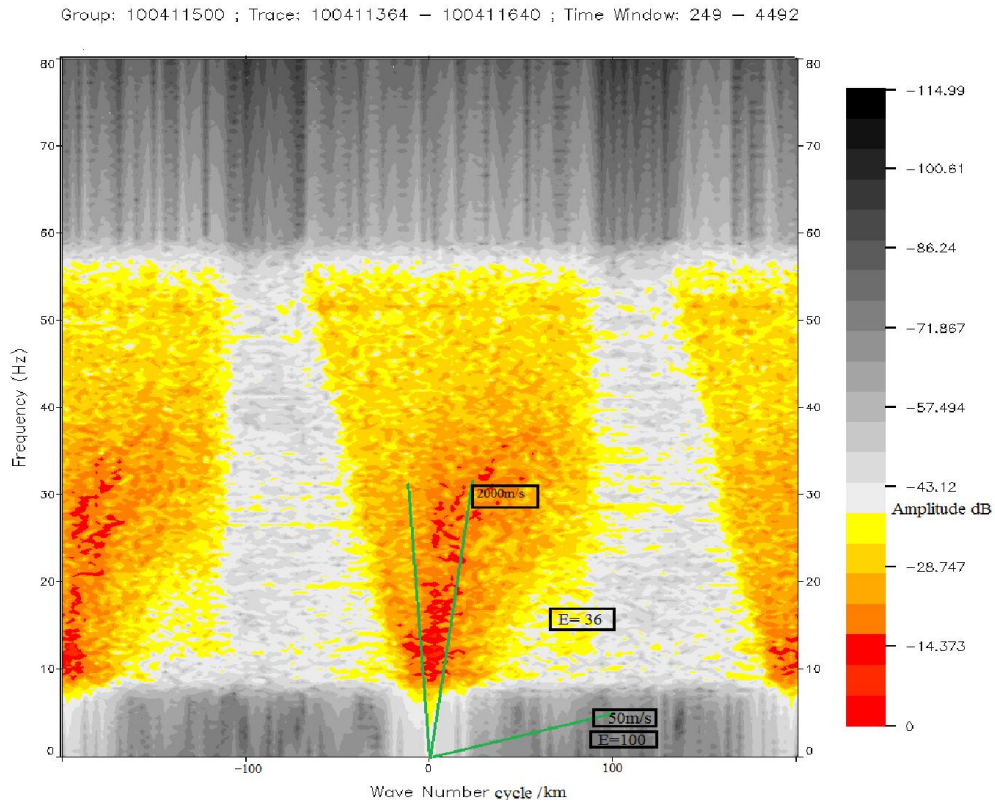


**Figure 3.25:**Raw shot 1004 Representation in the  $(f, k)$  domain

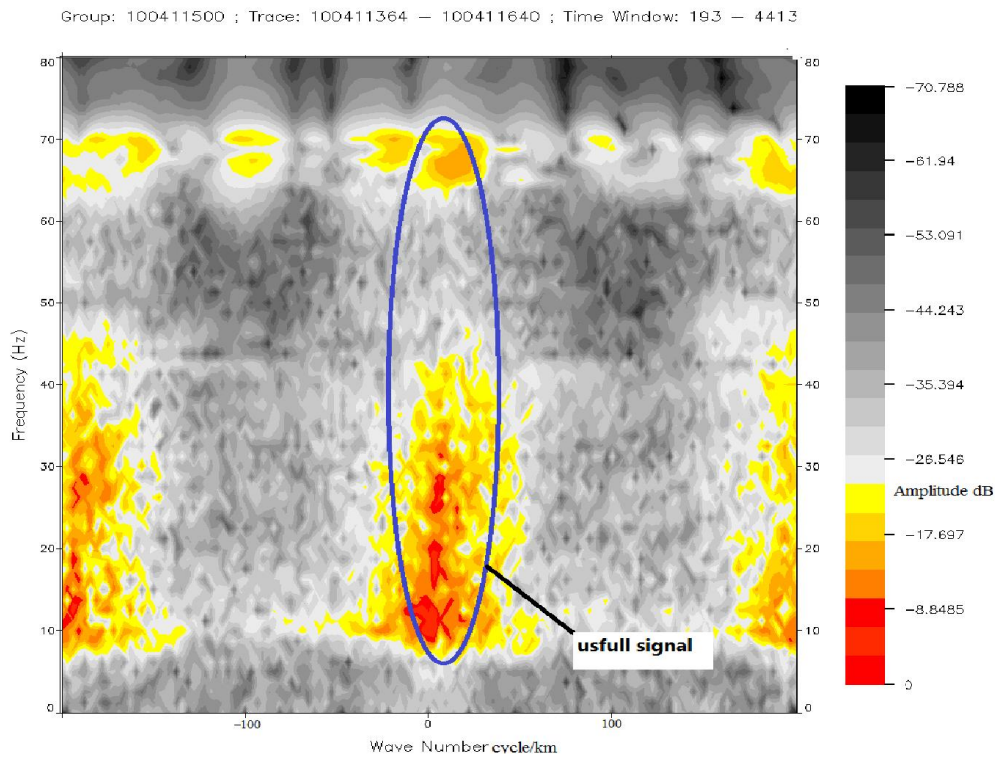


**Figure 3.26:**Shot after  $(f, k)$  filtering in  $(f, k)$  domain.



### 3.5.2. Ground roll Attenuation using AGORA:

The used parameters are:

- ✚ -The group velocity
- ✚ -The phase velocity
- ✚ -A frequency band
- ✚ The values are presented in the following table:

**Table 2: tested Parameters for AGORA.**

VGmin	VGmax	VPmin	VPmax	Fmin	Fmax
50	200	250	500	3	8
50	400	250	700	5	12
100	600	300	900	6	14
100	800	300	1200	7	15
150	1000	400	1500	8	15
150	1300	400	1800	9	17
150	1600	500	2200	10	18
200	1900	500	2500	10	20

#### 3.5.2.1. Result analysis and comparison:

- **On shot and stack:**

The analysis and comparison of the shot 1004 before and after the application of AGORA shows that the ground rolls are totally attenuated, and the hyperboles of the reflections are well identified on shot (see Figure 3.27 and 3.28). The results obtained on stack of the 16NG04 profile show that there are reflectors that was not visible before filtering the ground rolls with AGORA then they will become more visible on the stack which confirms the effectiveness of AGORA in the attenuation of the ground roll for the 16NG04 profile

(see Figure 3.31 and 3.32).

- **On spectrum:**

After analysis and comparison of the amplitude spectrum of shot 1004 before and after the AGORA application, we note that for the frequency band between 0 and 20 Hz amplitudes are greatly attenuated in parallel amplitudes in the band between 20Hz and 80Hz are slightly

attenuated (see Figure 3.31). After the various analyzes on shot and on stack we conclude that AGORA gives a good attenuation of the ground roll and improvement of the useful signal.

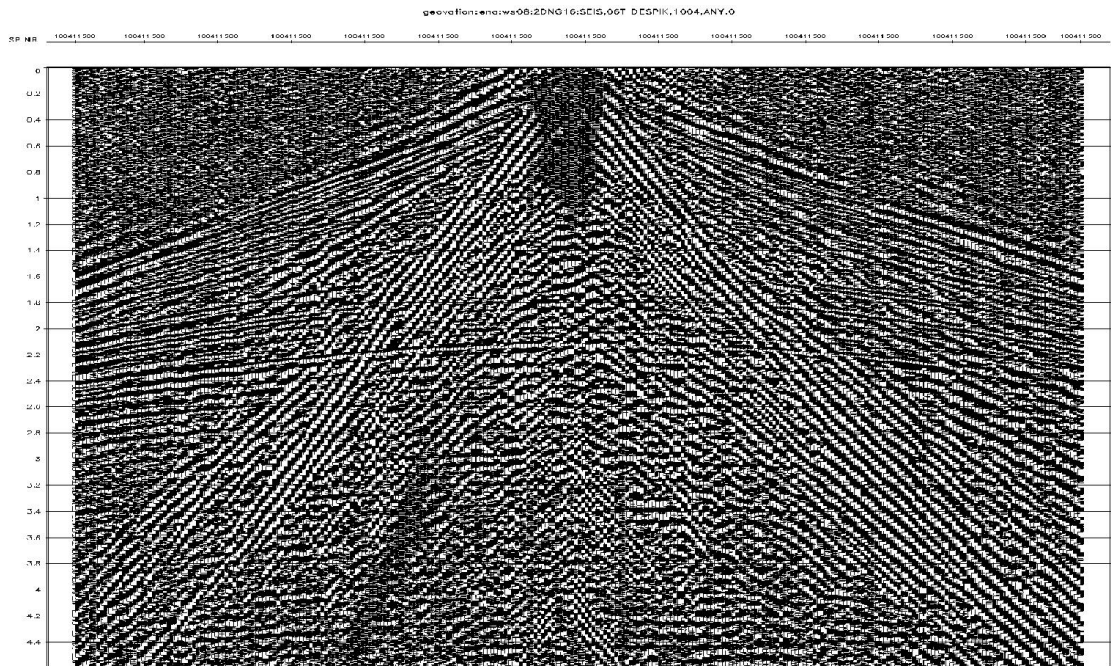


Figure 3.28: Shot 1004 before AGORA.

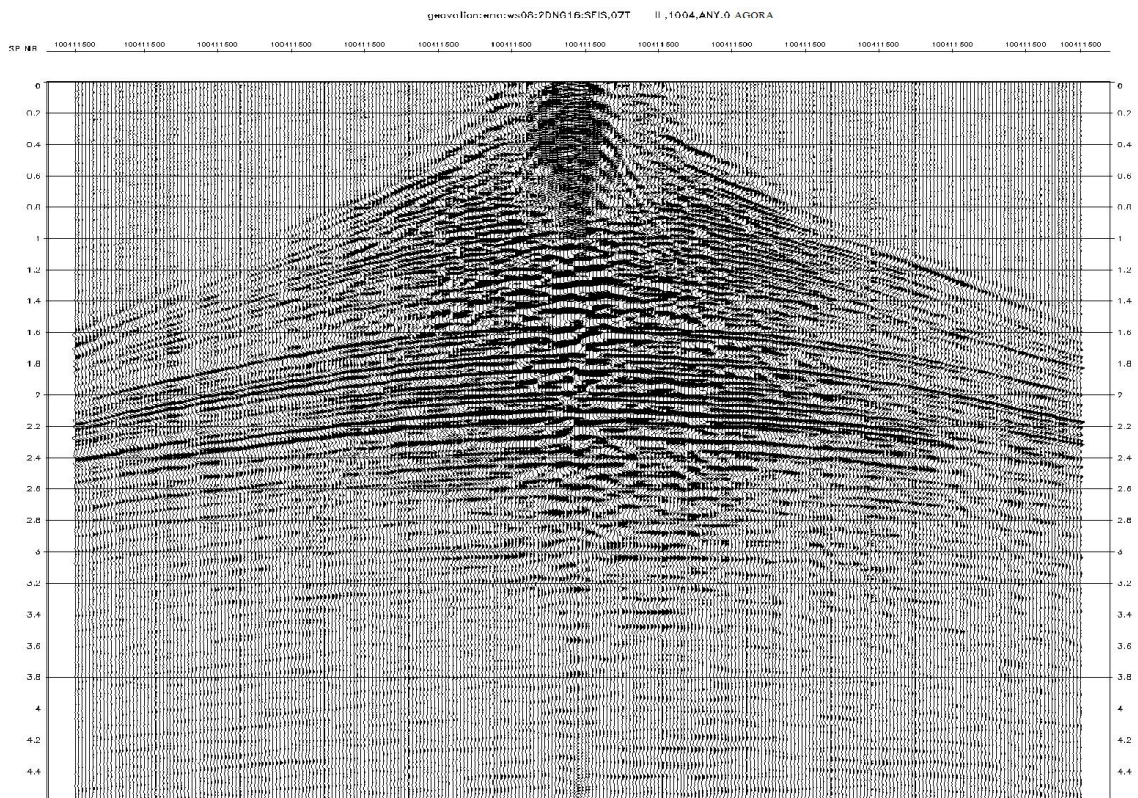


Figure 3.28: Shot after AGORA.



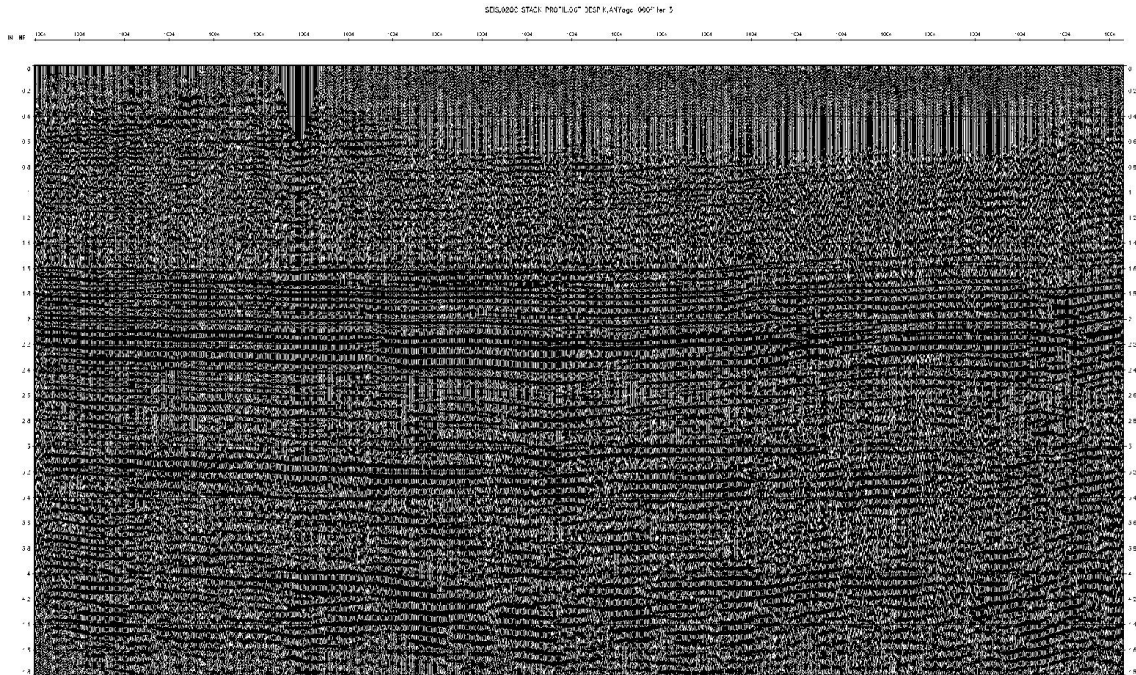


Figure 3.29: Stack before AGORA.

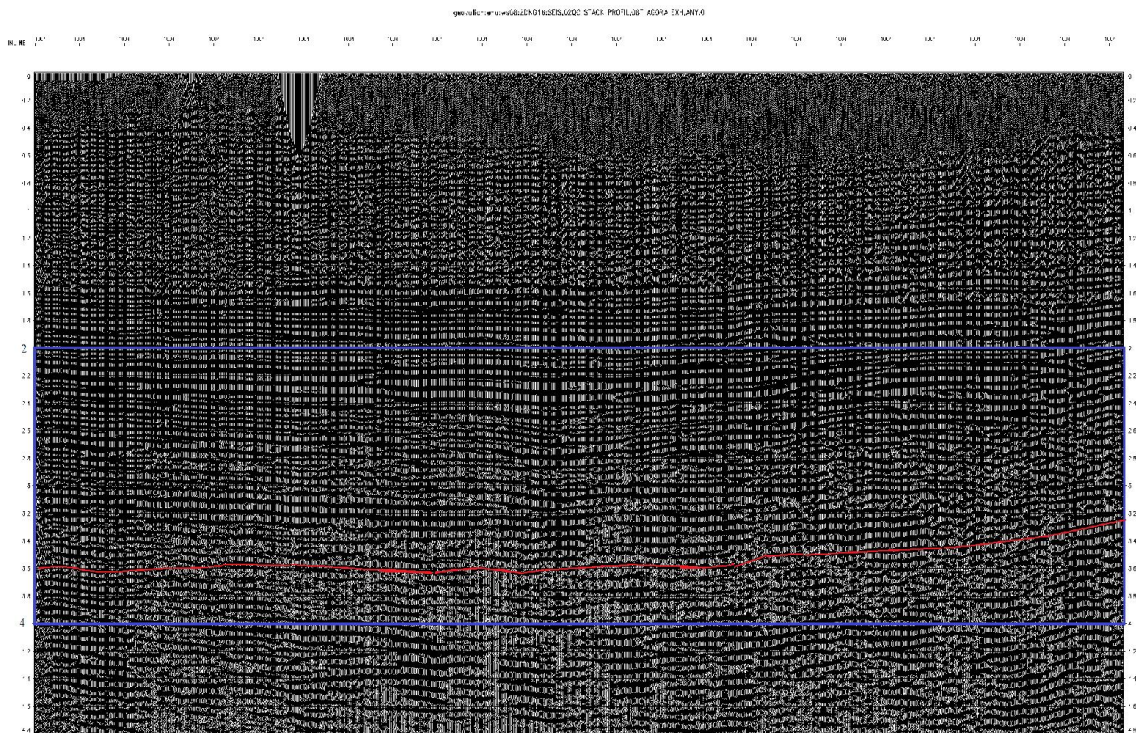


Figure3.30: Stack after AGORA.

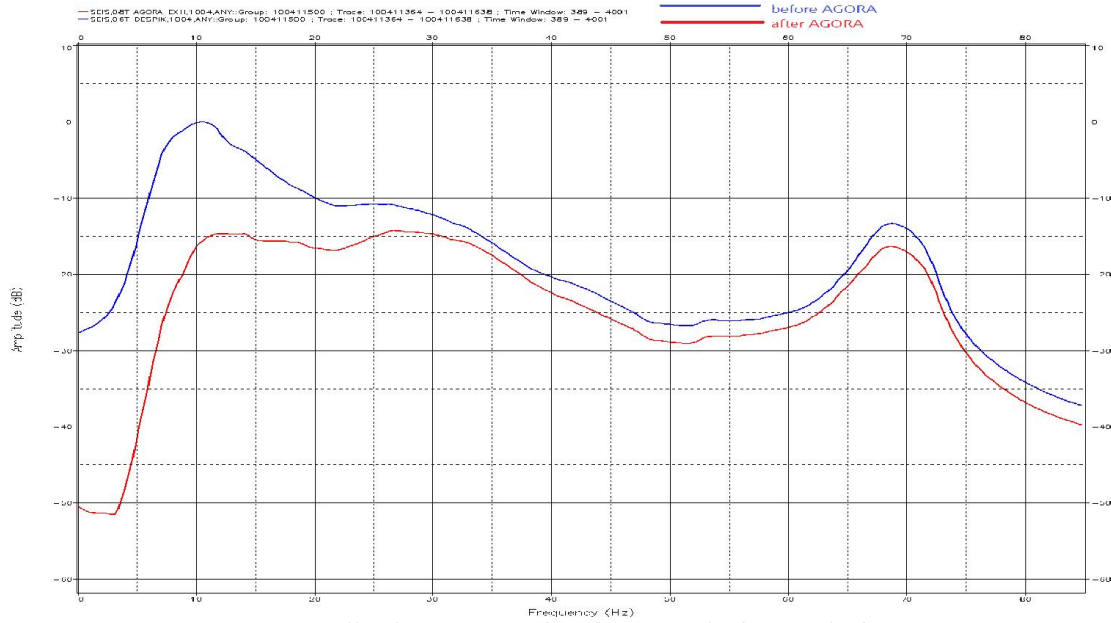


Figure 3.31: Amplitude spectrum for shot 1004 before and after AGORA.

### 3.6. Comparison between the two methods:

In this part, we compare the results obtained by the filter  $(f, k)$  and AGORA. The Figures: 3.32.a, 3.32.b, 3.33.a and 3.33.b show that ground rolls are attenuated by AGORA better than  $(f, k)$  filter. After analyzing the amplitude spectra of the shot 1004 using  $(f, k)$  filter and AGORA, we observe that for the frequency band between 0 and 25 Hz AGORA attenuated the amplitudes with a higher value than the  $(f, k)$  filter. On the other hand, in the frequency band between 25 and 80 Hz (the useful signal frequency band), the  $(f, k)$  filter attenuated the amplitudes with a higher value than AGORA (Figure 3.34). Based on that AGORA attenuates the ground roll and retains the useful signal with a great efficiency compared to the  $(f, k)$  filter (see Figure 3.35).



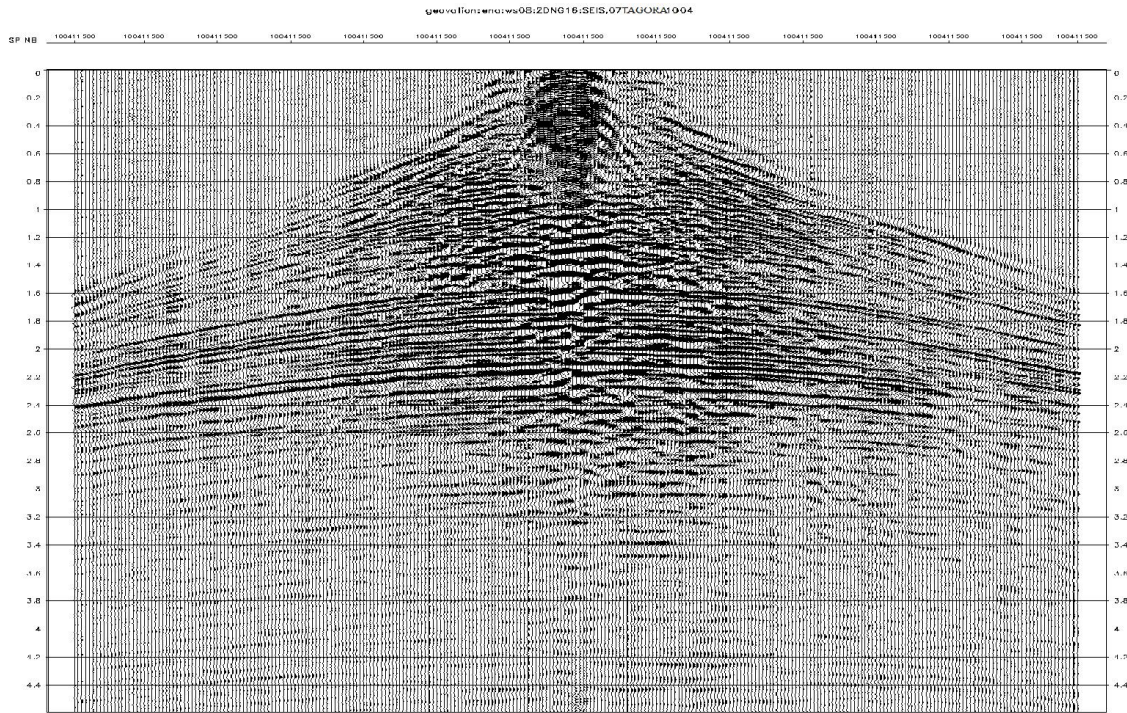


Figure 3.32.a: Shot 1004 After AGORA.

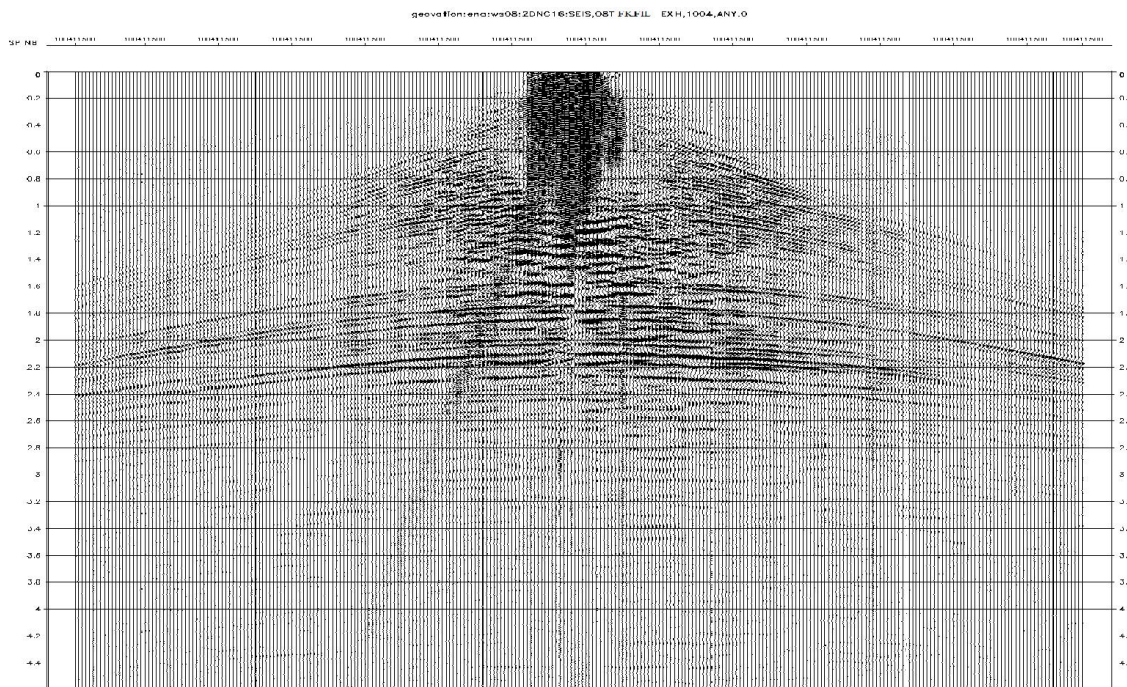


Figure 3.32.b: Shot 1004 after the application of (f, k) filter.



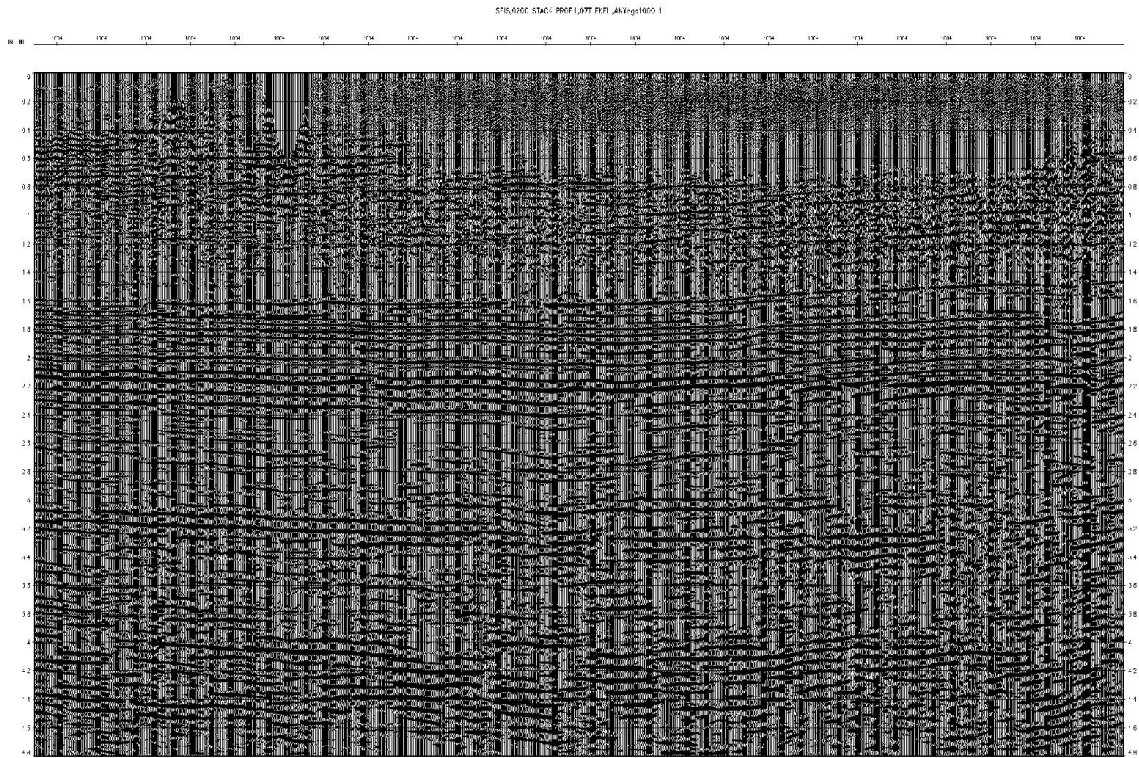


Figure 3.33.a:the stack of the profile 16NG04 after the application of (f; k) filter.

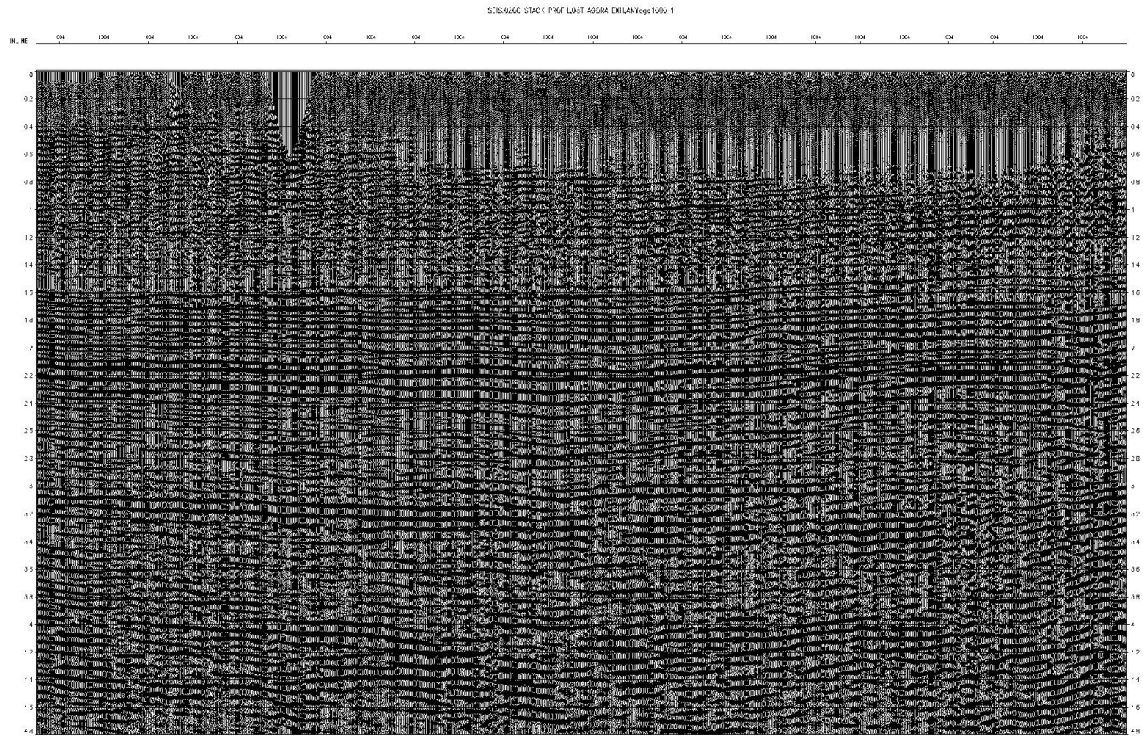


Figure 3.33.b: Stack of the profile 16NG04 after AGORA.

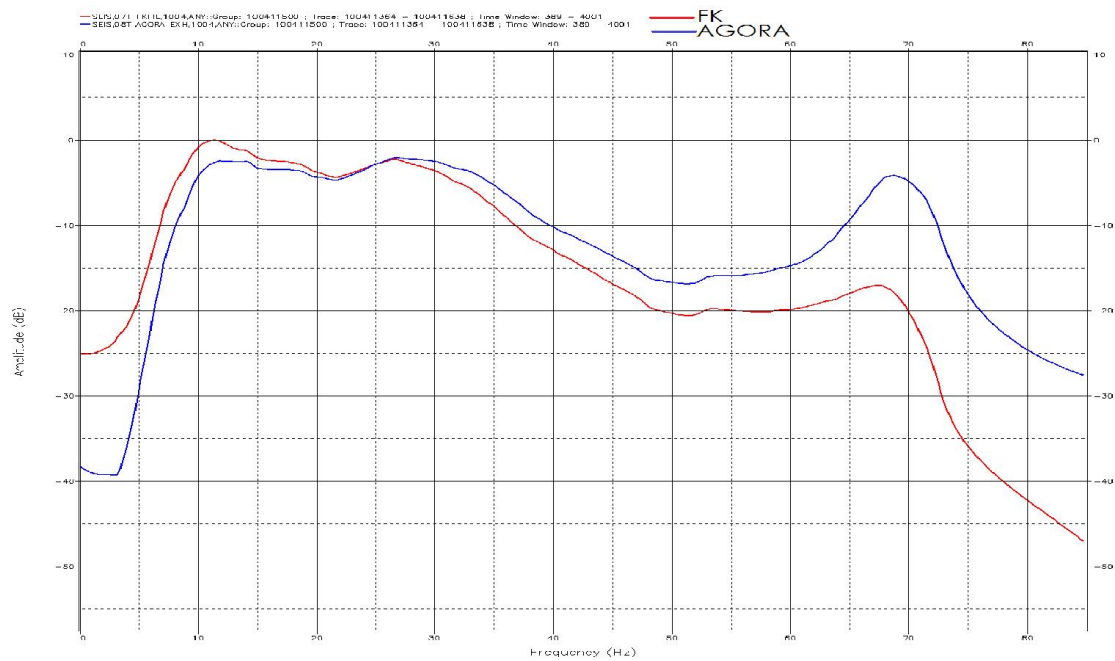
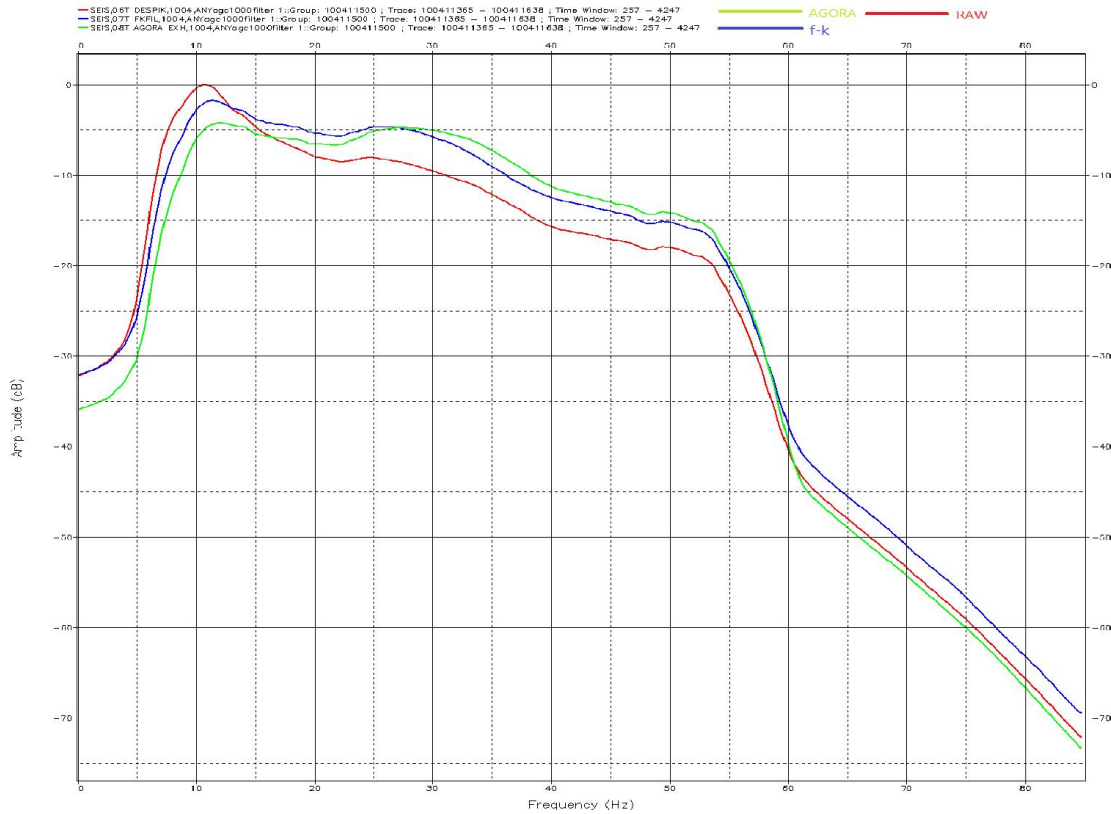


Figure 3.34: Amplitude spectra of shot 1004, after (f; k) filtering and after AGORA.





**Figure 3.35:** Amplitude spectra of the raw shot 1004, after (f, k) filtering and after AGORA.

figure3.35 demonstrates clearly that the AGORA filter attenuate the low frequency amplitudes(noisy frequency band) better than (F, K) filter and preserves the amplitudes with high frequency which contains the useful signal.

### 3.7.Summary:

The comparison of the results obtained from the attenuation of the parasitic signal (ground-roll) which affects the seismic recording by the filtering in the (f, k) domain and the AGORA modeling clearly shows the utility of the two methods, where the attenuation noise by AGORA is better than the attenuation by (f, k)filter. We have seen that these two filters are effective in filtering real data, and if they are well used, the results will be more accurate and then the interpretation of data will be easy. The application of our filter enabled us to separate the various events present well in the seismic recording, thus the filtering of the ground-roll.



## GENERAL CONCLUSION

Ground-roll attenuation is the concern of geophysicists, because it is the noise that masks almost completely the seismic information, for this reason seismic engineers have always sought to develop techniques to attenuate it as much as possible. The filtering of this noise by the  $(f, k)$  filtering and the AGORA modeling are techniques studied in this work.

At first, we gave an overview of the seismic acquisition, the seismic waves and the different phenomena that affect the seismic recording.

After having defined these signals on a seismic recording 2D, we focused our study on the elimination of certain signals called ground-roll which are presented as undesirable noise.

Noise attenuation, contained in seismic recordings acquired by surface-receiver-firing networks, two-dimensional filtering in the  $(f, k)$  domain, and AGORA modeling are techniques used at the processing center.

To be able to attenuate the ground-roll, in the case of 2D seismic study, it is imperative to attenuate the maximum of the random noises so that the two methods give reliable results. After comparing the results obtained by the two methods, we conclude that AGORA modeling is more effective for ground-roll attenuation compared to  $(f, k)$  filtering.

This work was for us of an immense contribution, since it contributed to especially enrich and apply the knowledge obtained during our course in a field as wide as signal processing.

At the end of this project we came up, with the following suggestions for further developments:

- Developing other types of filters in order to remove other types of noise: multiples, refractions waves...
- 3D Data processing.
- Seismic data processing using linear and nonlinear Radon Transform.

## Appendix A

### A.1. Reflection coefficients :

The equations of three different types of waves propagating in medium 1 and medium 2 are:

$$I(x,t) = I_0 e^{j\omega(t - \frac{x}{v_1})} \dots\dots\dots \text{incident wave}$$

$$R(x,t) = R_0 e^{j\omega(t - \frac{x}{v_1})} \dots\dots\dots \text{reflected wave}$$

$$T(x,t) = T_0 e^{j\omega(t - \frac{x}{v_1})} \dots\dots\dots \text{transmitted wave}$$

Where:

$I_0, R_0, T_0$  : are the amplitudes of the waves.

Knowing that:

$$I_0 + R_0 = T_0 \quad (A.1)$$

And having:  $R_0 = rI_0 \quad (A.2)$

$$T_0 = tI_0 \quad (A.3)$$

Applying the tension continuity law at the interface we get:

$$\rho_1 v_1 I_0 - \rho_1 v_1 R_0 = \rho_2 v_2 T_0 \quad (A.4)$$

Replacing (A.2)&(A.3) into (A.1) and (A.4) we get:

$$\begin{cases} \rho_1 v_1 (1 - r) = \rho_2 v_2 t \\ 1 + r = t \end{cases}$$

Solving the system with respect to  $r$  [6]:

$$r = \frac{\rho_1 v_1 - \rho_2 v_2}{\rho_1 v_1 + \rho_2 v_2} \quad (A.5)$$

In function of  $z$  :

$$r = \frac{z_1 - z_2}{z_1 + z_2} \quad (A.6)$$

### A.2. Spatial filtering:

$$\begin{aligned}
 FT \left[ \sum_{i=0}^N \delta(x - ie) \right] &= \sum_{n=0}^N e^{-j 2\pi nke} \\
 &= 1 + e^{-j 2\pi ke} + e^{-j 4\pi ke} + \dots + e^{-j 2\pi Nke} \\
 &= \frac{1 - e^{-j 2\pi Nke}}{1 - e^{-j 2\pi ke}}
 \end{aligned}$$

In modulus we get:

$$\left| \frac{1 - e^{-j 2\pi Nke}}{1 - e^{-j 2\pi ke}} \right| = \frac{|1 - e^{-j 2\pi Nke}|}{|1 - e^{-j 2\pi ke}|}$$

1)

$$\begin{aligned}
 |1 - e^{-j 2\pi Nke}| &= |e^{-j \pi Nke} (e^{j \pi Nke} - e^{-j \pi Nke})| \\
 &= 2 |\sin(\pi kNe)|
 \end{aligned}$$

2)

$$\begin{aligned}
 |1 - e^{-j 2\pi ke}| &= |e^{-j \pi ke} (e^{j \pi ke} - e^{-j \pi ke})| \\
 &= 2 |\sin(\pi ke)|
 \end{aligned}$$

Yields:

$$FT \left[ \sum_{i=0}^N \delta(x - ie) \right] = \frac{|\sin(\pi kNe)|}{|\sin(\pi ke)|} \quad (A.7)$$

## Appendix B:

## B.1. Fourier Transform:

### B.1.1. 1D Fourier Transform:

The passage from the time field to the frequency field is ensured by the Fourier transform which by definition:

$$FT[s(t)] = S(f) = \int_{-\infty}^{+\infty} s(t) e^{-j2\pi ft} dt \quad (B.1)$$

The inverse Fourier transform  $FT^{-1}$  ensure the passage from the frequency field to the time field by this relation:

$$FT^{-1}[S(f)] = s(t) = \int_{-\infty}^{+\infty} S(f) e^{+j2\pi ft} df \quad (B.2)$$

### B.1.2. 1D Discrete Fourier Transform:

The discrete Fourier transform DFT is defined as follows:

$$DFT[s(n_t)] = \sum_{n_t=0}^{N_t-1} s(n_t) e^{\frac{-j2\pi n_t n_f}{N_t}} \quad (B.3)$$

And the inverse of the DFT is:

$$DFT^{-1}[S(n_f)] = \frac{1}{N_t} \sum_{n_f=0}^{N_f-1} S(n_f) e^{\frac{+j2\pi n_t n_f}{N_t}} \quad (B.4)$$

Where:

$n_t, n_f$  : the sample number in time and frequency respectively.

$N_t, N_f$  : the number of samples in time and frequency respectively.

Note that the number of samples in time is equal to the number of samples in frequency.

### B.1.3. 2D Fourier transform:

It is a double application of the Fourier transform. Thus for a function  $s(t, x)$  ; by definition the double Fourier transform of this function is:

$$FT[s(t, x)] = FT_x\{FT_t[s(t, x)]\} = \int_{-\infty}^{+\infty} \int_{-\infty}^{+\infty} s(t, x) e^{-j2\pi(ft+kx)} dt dx = S(f, k) \quad (B.5)$$

The inverse 2D Fourier transform  $BFT^{-1}$  as follows:

$$s(t, x) = \int_{-\infty}^{+\infty} \int_{-\infty}^{+\infty} S(f, k) e^{+j2\pi(ft+kx)} df dk \quad (B.6)$$

### B.1.4. 2D Discrete Fourier Transform:

The bidimensional discrete Fourier transform BDFT is defined by the relation[7]:

Forward:

$$S(n_k, n_f) = \sum_{n_x=0}^{N_x-1} \sum_{n_t=0}^{N_t-1} s(n_x, n_t) e^{-j2\pi \left[ \frac{n_x n_k}{N_x} + \frac{n_t n_f}{N_t} \right]} \quad (B.7)$$

Where:

$n_t, n_f, n_x, n_k$ : The sample number in time, in frequency, in distance and wavenumber respectively.

$N_t, N_x$ : The number of samples in time and frequency respectively.

Inverse[7]:

$$s(n_x, n_t) = \frac{1}{N_x N_t} \sum_{n_k=0}^{N_k-1} \sum_{n_f=0}^{N_f-1} S(n_k, n_f) e^{-j2\pi \left[ \frac{n_x n_k}{N_x} + \frac{n_t n_f}{N_t} \right]} \quad (B.8)$$

$N_k, N_f$ : represent respectively the number of samples in wave-number and in frequency.

## B.2. Sampling:

Sampling is the process of obtaining DTS from CTS because analysis and design use digital techniques. The product  $h(t) \cdot \delta_{T_s}(t)$  is a distribution; it takes a value  $h(nT_s)$  for  $t = nT_s$  and is zero for  $t \neq nT_s$ .

$$h(t) \delta_{T_s}(t) = \sum_{n=-\infty}^{+\infty} h(nT_s) \delta_{nT_s} \quad (B.9)$$

By expressing the FT of a product:

$$FT \left[ h(t) \cdot \delta_{T_s}(t) \right] = \frac{1}{T_s} H(f) * \delta_{\frac{1}{T_s}}(f) = \frac{1}{T_s} \sum_{n=-\infty}^{+\infty} H(f - \frac{n}{T_s}) \quad (B.10)$$

## B.3. Shannon theorem:

Because sampling the spectrum  $H(f)$  makes it become periodic, the spectrum of  $H(f)$  is conserved if the Shannon criterion is met, that is  $f_s > 2f_{\max}$ . the maximum frequency  $f_{\max}$  is the limit such that the amplitude spectrum of  $H(f)$  is zero for frequencies higher than  $f_{\max}$ . the interval  $[-f_{\min}, +f_{\max}]$  is called the non-zero region (NZR) of  $H$ .

The frequency limit that must not exceed  $f_{\max}$  is called the Shannon frequency or Nyquist frequency.

## B.4. Properties of 1D Fourier transform:

Properties	Signals	Fourier transform
Definition	$s(t)$	$S(f)$
Linearity	$s_1(t) + s_2(t)$	$S_1(f) + S_2(f)$
Time shifting	$s(t - t_0)$	$S(f) e^{-j 2 \pi f t_0}$
Frequency shifting	$s(t) e^{-j 2 \pi f_0 t}$	$S(f - f_0)$
Time convolution	$s(t) * w(t)$	$S(f) W(f)$
Frequency convolution	$s(t) . w(t)$	$S(f) * W(f)$
Scaling theorem	$s(at)$	$\frac{1}{ a } S(\frac{f}{a})$
Differentiation	$d^n s(t) / dt^n$	$(j 2 \pi f)^n S(f)$
Integration	$\int_{-\infty}^t s(t) dt$	$\frac{1}{j 2 \pi f} S(f) + \frac{1}{2} S(0) \delta(f)$
Parseval's theorem	$\int_{-\infty}^{+\infty}  s(t) ^2 dt = \int_{-\infty}^{+\infty}  S(f) ^2 df$	

### B.5. Properties of 2D Fourier transform:

Properties	Signals	Fourier transform
Definition	$s(t, x)$	$S(f, k)$
Time shifting	$s(t - t_0, x)$	$e^{-j 2 \pi k t_0} S(f, k)$
Spatial shifting	$s(t, x - x_0)$	$e^{-j 2 \pi k x_0} S(f, k)$
Scaling theorem	$s(at, bx)$	$\frac{1}{ ab } S(\frac{f}{a}, \frac{k}{b})$
temporal Differentiation	$\frac{d^n s(t, x)}{dt^n}$	$(j 2 \pi f)^n S(f, k)$
Special differentiation	$\frac{d^n s(t, x)}{dx^n}$	$(j 2 \pi k)^n S(f, k)$

## **BIBLIOGRAPHY**

- [1] F.Lechani, M. Bouaziz, «**Teste et optimisation des paramètres d'acquisition 3-D**»mémoire fin de formation d'ingénieur spécialisé en géophysique IAP / E.N.A.GEO
- [2] M.S.Rouifed, R.Tiguerchah, «**Filtrage numérique des bruits cohérent (Ground-roll) en sismique pétrolière 2D avec les filtres (f,k) et (tau,p)** »
- [3] D.S. Parasnis«**Principle of applied geophysics**» Book edition technip1993.
- [4] J.L. MARI, G.Arens, D.Chapellier, P.Gaudian, «**Géophysique de gisement et de génie civil** »Book edition technip1993.
- [5] AP/ IB GEOGRAPHY 2017, <http://volcanoesmakemeexplode.wikifoundry.com/>.
- [6] George Nely,«**Evaporite sequences in petroleum exploration**»Vol.2(geophysical methods)Book edition technip1994.
- [7] J.L.Mari, F.Glangeaud, F.Coppens, «**Signal processing for geologists & geophysicists**»
- [8] Reeshidev Bansal and Matthias G. Imhof - Diffraction enhancement in prestack seismic data.
- [9] ENVIROSCAN INC 2018, SURFACE GEOPHYSICS TECHNIQUES, viewed 20 April 2018, <http://www.enviroscan.com/techniques-applications-land>.
- [10] Schlumberger2018,Oilfield Glossary, viewed 10 April 2018, <http://www.glossary.oilfield.slb.com>
- [11] Zhu, X. S., Gao, R., Li, Q. S., et al., 2014. Static Corrections Methods in the Processing of Deep Reflection Seismic Data. Journal of Earth Science, 25(2): 299–308, doi:10.1007/s12583-014-0422-x
- [12] GeoSci Developers 2017, Seismic, viewed 5 march 2018, <http://www.bairdpetro.com/>
- [13] PROFESSIONAL GEOPHYSICS 2018, Seismic Analysis and Detail, viewed 10 mars 2018, <http://www.bairdpetro.com/>.
- [14] Wikipedia 2018 , Seismic migration, viewed 5 march 2018, [https://en.wikipedia.org/wiki/Seismic\\_migration](https://en.wikipedia.org/wiki/Seismic_migration).
- [15] Perkins, C. and Zwaan, M. Ground roll attenuation.70th EAGE Conference & Exhibition — Rome, Italy, 9 - 12June 2008.